

การติดตามแนวรอยเลื่อนสะแกงในประเทศพม่าด้วยข้อมูลจีพีเอส

นายปิย์ โสณ อ่อง



จุฬาลงกรณ์มหาวิทยาลัย
CHULALONGKORN UNIVERSITY

บทคัดย่อและแฟ้มข้อมูลฉบับเต็มของวิทยานิพนธ์ตั้งแต่ปีการศึกษา 2554 ที่ให้บริการในคลังปัญญาจุฬาฯ (CUIR)

เป็นแฟ้มข้อมูลของนิสิตเจ้าของวิทยานิพนธ์ ที่ส่งผ่านทางบัณฑิตวิทยาลัย

วิทยานิพนธ์นี้เป็นส่วนหนึ่งของการศึกษาตามหลักสูตรปริญญาวิทยาศาสตรมหาบัณฑิต

The abstract and full text of theses from the academic year 2011 in Chulalongkorn University Intellectual Repository (CUIR) are the thesis authors' files submitted through the University Graduate School.

สาขาวิชาวิศวกรรมสำรวจ ภาควิชาวิศวกรรมสำรวจ
คณะวิศวกรรมศาสตร์ จุฬาลงกรณ์มหาวิทยาลัย

ปีการศึกษา 2557

ลิขสิทธิ์ของจุฬาลงกรณ์มหาวิทยาลัย

Monitoring of the Sagaing fault in Myanmar using GPS observations

Mr. Pyae Sone Aung



A Thesis Submitted in Partial Fulfillment of the Requirements
for the Degree of Master of Engineering Program in Survey Engineering

Department of Survey Engineering

Faculty of Engineering

Chulalongkorn University

Academic Year 2014

Copyright of Chulalongkorn University

ปิย โสณ อ่อง : การติดตามแนวรอยเลื่อนสะแกงในประเทศพม่าด้วยข้อมูลจีพีเอส (Monitoring of the Sagaing fault in Myanmar using GPS observations) อ.ที่ปรึกษาวิทยานิพนธ์หลัก: ศ. ดร.เฉลิมชนม์ สติระพจน์, 88 หน้า.

วัตถุประสงค์ของงานวิจัยนี้เพื่อทำการประมวลผลโครงข่ายหมุดดาวเทียม GPS ของสาธารณรัฐแห่งสหภาพเมียนมาร์ โดยอาศัยการประมวลผลบนซอฟต์แวร์ GAMIT และ GLOBK เพื่อให้ได้ทิศทางและอัตราการเคลื่อนตัวของทุกจุดของค่าพิกัดของสถานีรับสัญญาณดาวเทียม GPS และทำการติดตามการเคลื่อนตัวของเปลือกโลกขณะเกิดแผ่นดินไหว โดยใช้ซอฟต์แวร์ TRACK kinematic processing โดยในงานวิจัยนี้ใช้ข้อมูล GPS ที่ทำการรวบรวมได้ ในช่วงระยะเวลา 4 ปี ระหว่างปี 2011-2014 ซึ่งค้นพบว่าด้านตะวันออกของรอยเลื่อน sagaing มีการเคลื่อนตัวไปในทิศตะวันออกเฉียงใต้ ด้วย อัตราการเคลื่อนตัวประมาณ 32 - 40 มม. ต่อปี ส่วนอีกด้านหนึ่งของรอยเลื่อนมีการเคลื่อนตัวไปในทิศตะวันออกเฉียงเหนือด้วยอัตราการเคลื่อนตัวประมาณ 31-35 มม. ต่อปี สำหรับการศึกษากการเคลื่อนตัวของเปลือกโลกในงานวิจัยนี้ได้ข้อมูลมาจากโครงข่ายหมุดดาวเทียม GPS ของ ประเทศ สาธารณรัฐแห่งสหภาพเมียนมาร์ 2 สถานี ที่อยู่ในบริเวณที่มีความเกี่ยวข้องกับการเกิดแผ่นดินไหว Thebeikkyin ในปี 2012 ซึ่งมีขนาด 6.8 แมกนิจูด โดยสถานีรับสัญญาณดาวเทียม GPS ตั้งอยู่ห่างจากศูนย์กลางของแผ่นดินไหวประมาณ 50-60 กิโลเมตร จาก ข้อมูล ที่ได้ จาก การ รัง วัด สัญญาณ GPS แสดงให้เห็นถึงการเคลื่อนตัวของเปลือกโลกซึ่งมีการเปลี่ยนแปลงตัวในแนวราบ จากผลของการประมวลผลด้วยวิธี Kinematic ค่าพิกัดของสถานีรับสัญญาณดาวเทียม GPS ทางด้านทิศตะวันออกของรอยเลื่อน sagaing มีการเคลื่อนตัวไปในทิศใต้ 15 ซม. และเคลื่อนตัวไปทางทิศเหนือ 3 ซม. อย่างทันทีทันใด โดยในการศึกษานี้จะทำการเปรียบเทียบผลที่ได้จากการประมวลผลด้วยวิธี kinematic เพื่อทำการศึกษาหาอัตราการเคลื่อนตัวของเปลือกโลกหลังจากการเกิดแผ่นดินไหว และ ผลลัพธ์ ของ อนุกรม เวลา ที่ได้ จาก ซอฟต์แวร์ GAMIT และ GLOBK ซึ่งผลลัพธ์ที่ได้มีความสอดคล้องกันอย่างมีนัยสำคัญ จากการศึกษาสามารถสรุปได้ว่าเราสามารถเฝ้าระวังการเคลื่อนตัวของรอยเลื่อน sagaing โดยใช้ข้อมูลที่ได้จากการรังวัดสัญญาณ GPS และรูปแบบการเคลื่อนตัวของรอยเลื่อนที่บันทึกมา เพื่อใช้ในการประมวลผลได้ ซึ่งการประมวลผลด้วยวิธีนี้จะป็นประโยชน์ในการทำการศึกษวิจัยและบันทึกรูปแบบการเคลื่อนตัวของรอยเลื่อน sagaing ในประเทศสาธารณรัฐแห่งสหภาพเมียนมาร์ ต่อไป

ภาควิชา วิศวกรรมสำรวจ

ลายมือชื่อนิสิต

สาขาวิชา วิศวกรรมสำรวจ

ลายมือชื่อ อ.ที่ปรึกษาหลัก

ปีการศึกษา 2557

5670483921 : MAJOR SURVEY ENGINEERING

KEYWORDS: THE SAGAING FAULT, GPS, GAMIT AND GLOBK

PYAE SONE AUNG: Monitoring of the Sagaing fault in Myanmar using GPS observations. ADVISOR: PROF. CHALERMCHON SATIRAPOD, Ph.D., 88 pp.

The objectives of the research were to analyze the Myanmar cGPS network observations to obtain a moving rate and direction of every cGPS point by using the GAMIT and GLOBK software package and to investigate the co-seismic moving rate due to the earthquake by using the TRACK kinematic processing program. The study observed four years of continuous GPS data between 2011 and 2014. It was found that the east side of the Sagaing fault the moving toward the southeast with the average rate of approximately 32-40 mm/yr and the other side of the fault the moving to the northeast with the rate of about 31-35 mm/yr. For the co-seismic study were observed at 2 stations of the Myanmar cGPS network, associated with the 2012 M6.8 Thebeikkyin earthquake. The GPS stations are located 50-60 km away from the epicenter. The GPS observation data clearly showed co-seismic ground displacements. According to the kinematic processing results, the GPS station from the east side of the Sagaing fault immediately moves to the southward, offset rate is 15 cm. Other side of the GPS station north offset is 3 cm. This study was compared the kinematic processing results for co-seismic movement rate and GAMIT/GLOBK time series results, which showed fairly good agreements. From this study, it can be concluded that the Sagaing fault using the GPS observation, the Sagaing fault's tectonic activities can be monitored. This analysis method is useful in many ways to make a research on monitoring the Sagaing fault tectonic actives in Myanmar.

Department: Survey Engineering

Student's Signature

Field of Study: Survey Engineering

Advisor's Signature

Academic Year: 2014

ACKNOWLEDGEMENTS

Firstly, I strongly wish to express my special thanks to my advisor Professor Dr. Chalermchon Satirapod, from the Department of Survey Engineering, Faculty of Engineering, Chulalongkorn University, who shared his knowledge and experience with me. Then, I would like to show a great thank to the stakeholders of Chulalongkorn University Scholarship Program for ASEAN Countries. I am deeply appreciative of your support. I would like to thank to Daw Hla Hla Aung and U Soe Thura Tun who are gave me precious suggestion throughout this thesis work. I am indebted to Myanmar Earthquake Committee (MEC) and Earth Observatory of Singapore (EOS) who provided me all the GPS data and software. I would like to acknowledge and extend my heartfelt gratitude to the committee members; Associate Professor Dr. Chanin Tinnachote, Dr. Thongthit Chayakula and Dr. Teetat Charoenkalunyuta, who contributed to improvement of my thesis by critical comments.

I would like to show a great thank to my parents, Eint Thu Htet, family of my elder sisters and younger brother for their support and encouragement through my life. At the end, I am grateful to all who contributed to this work.

CONTENTS

	Page
THAI ABSTRACT	iv
ENGLISH ABSTRACT	v
ACKNOWLEDGEMENTS	vi
CONTENTS	vii
LIST OF TABLES	x
LIST OF FIGURES	xi
CHAPTER 1 INTRODUCTION	1
1.1 Statement of Problem	1
1.2 Objectives	2
1.3 Scope of Investigation	2
1.4 Expected Contribution	3
CHAPTER 2 THEORY AND LITERATURE REVIEW	4
2.1 The Sagaing Fault	4
2.2 The GPS Overview	7
2.1.1 GPS for Geodetic Measurements	7
2.1.2 The GPS System	8
2.1.3 Space Segment	8
2.1.4 Control Segment	9
2.1.5 User Segment	9
2.1.6 The Ground Segment	10
2.1.7 The GPS Signals	10
2.1.8 The GPS observables	11

	Page
2.1.9 Observable in Data Processing.....	12
2.1.10 Linear Combinations of Observations	17
2.1.11 International Terrestrial Reference Frame (ITRF).....	19
2.1.12 Reference Stations.....	19
2.3 Literature Review.....	20
CHAPTER 3 METHODOLOGY AND DATA PROCESSING	23
3.1 Methodology.....	23
3.2 Introduction to Myanmar cGPS network.....	24
3.3 Equipment and Site Monumentation	27
3.4 Data collection and preparation.....	28
3.5 Data Processing.....	31
3.5.1 Overview of GAMIT Processing.....	31
3.5.2 GAMIT processing.....	31
3.5.3 Automatic Batch Processing with GAMIT.....	35
3.5.4 Evaluating of the results.....	37
3.5.5 Overview of the GLOBK Processing.....	37
3.5.6 Preparing the input files for The GLOBK.....	37
3.5.7 Overview of the GGMatlab.....	39
3.5.8 Kinematic Track Processing.....	40
CHAPTER 4 RESULTS AND DISCUSSION	43
4.1. Myanmar cGPS Network Time series results and Discussion.....	43
4.2. Comparing GPS results and discussion.....	48
4.3. Measuring Displacement due to the Thabeikkyin Earthquake	50

	Page
4.4. Velocity Vector	51
4.5. Kinematic Processing Results and discussion.....	53
CHAPTER 5 CONCLUSIONS AND RECOMMENDATION FOR FURTHER STUDY	56
5.1. Conclusion	56
5.2. Recommendation for Further Study	57
REFERENCES	58
APPENDIX.....	64
VITA.....	88



LIST OF TABLES

Table 3-1 List of the Myanmar cGPS stations, Instrument type, coordinates and station to station distance.....	25
Table 3-2 Myanmar cGPS stations observation data set used in this research.....	29
Table 4-1 Moving rate of Myanmar cGPS network.....	51
Table 4-2 Based on time series results determine the moving rate of GPS stations.....	52



LIST OF FIGURES

Figure 2.1 Tectonic features of Myanmar and surrounding areas (Modified after (Morley 2004, Mitchell, Htay et al. 2007, Searle and Morley 2011, Watkinson, Elders et al. 2011, Tun and Thein 2012, Ridd and Watkinson 2013)).....	6
Figure 2.2 The GPS nominal constellation (Dana 2000)	9
Figure 2.3 The GPS satellite signals (Dana 2000).....	11
Figure 2.4 measuring the pseudorange (Langley 1997)	12
Figure 2.5 Two receivers P and Q observe one satellite A.....	13
Figure 2.6 One receiver P observe two satellites A and B.....	14
Figure 2.7 Two receivers P and Q observe two satellites A and B	16
Figure 2.8 Mandalay transects stations (Vigny, Socquet et al. 2003).....	21
Figure 3.1 Methodological flow chart of GPS data processing (using with GAMIT and GLOBK software).....	24
Figure 3.2 IGLE GPS station Antenna (Trimble choke ring type antenna).....	26
Figure 3.3 IGLE GPS station receiver box (Trimble NetR8 GNSS receiver).....	26
Figure 3.4 Myanmar permanent cGPS stations Location map. HAKA, KANI, SWBO and SDWN are northern transect of Myanmar cGPS network. GYBU, IGLE, WAAW and SATG are southern transect of Myanmar cGPS network.....	27
Figure 3.5 Design for monumentation, steel tripod used in Myanmar cGPS network.....	28
Figure 3.6 Map of the IGS stations which have been used in the Myanmar cGPS network processing	30
Figure 3.7 Directories structure, create working directories before processing.....	32

Figure 3.8 Example of a tsviews screen image.....	40
Figure 3.9 Epicenter location map of the M 6.8 Thabeikkyin Earthquake in Myanmar (23.005°N 95.885°E)	41
Figure 4.1 Time series of the Myanmar continuous GPS station (GYBU).....	44
Figure 4.2 Time series of the Myanmar continuous GPS station (IGLE).....	45
Figure 4.3 Time series of the Myanmar continuous GPS station (WAAW).....	45
Figure 4.4 Time series of the Myanmar continuous GPS station (SATG)	46
Figure 4.5 Time series of the Myanmar continuous GPS station (HAKA).....	46
Figure 4.6 Time series of the Myanmar continuous GPS station (KANI)	47
Figure 4.7 Time series of the Myanmar continuous GPS station (SWBO).....	47
Figure 4.8 Time series of the Myanmar continuous GPS station (SDWN).....	48
Figure 4.9 Comparing two stations time series (between the SATG and WAAW stations).	49
Figure 4.10 Comparing two stations time series (between the IGLE and GYBU stations).	49
Figure 4.11 Comparing three stations time series (between the HAKA, KANI and SWBO stations).	50
Figure 4.12 Example plot for the SWBO station	52
Figure 4.13 Velocity map for the Myanmar cGPS network	53
Figure 4.14 Kinematic processing result of SDWN station.....	54
Figure 4.15 Kinematic processing result of SWBO station.....	54

CHAPTER 1

INTRODUCTION

1.1 Statement of Problem

All the plates on the surface of the Earth have moved with constant motion rates. These motions can be measured by different ways of measurement techniques. One of the techniques is a space-based geodetic measurement. Geodesy is the science, which is measuring the size and shape of the Earth (Vaniček and Krakiwsky 1986). During the past decade, the precise geodetic measurement method of the NAVSTAR Global Positioning System (GPS) has become world-wide acceptance for monitoring tectonic phenomena. The GPS measurement system can provide millimeter-level positioning accuracy which allows studying in tectonic movements (McClusky, Balassanian et al. 2000, Vigny, Chery et al. 2002, McClusky, Reilinger et al. 2003, Reilinger, McClusky et al. 2006).

Myanmar, the second-largest country in Southeast Asia, lies in the westernmost part of the Sunda megathrust and Myanmar also counts two more fault systems that conform to the northward translation of India on the Sunda block (Wang, Shyu et al. 2013). The Sagaing fault is one of the major active faults in Myanmar, more than 1,200 kilometers in length. As the Sagaing fault had experienced many earthquakes in her history and as the major cities are along the active faults, especially Sagaing fault, the seismic studies are critically important.

The Sagaing fault is a right lateral strike-slip fault (Curry, Moore et al. 1979, Bird 2003, Curry 2005). There have been studies of the Sagaing fault to get slip rate. Vigny (2003) measured the Sagaing fault slip rate by using campaign GPS observations. According to the Vigny (2003) result, The Sagaing fault slip rate is 18mm/yr (Vigny, Socquet et al. 2003). Wang and Sieh (2011) whose are scientists at the Earth Observatory of Singapore (EOS) have measured a slip rate on the strike-slip Sagaing fault of 11-18 mm/yr (Wang, Sieh et al. 2011).

Nevertheless, although previous studies work has been done to get the Sagaing fault slip rate, more studies need to be conducted to obtain a slip rate. The present

study was used the continuous (permanent) GPS stations to monitor the tectonic deformation of the Sagaing fault. This cGPS provides station motion at the better precision. Therefore, investigating the tectonic activity of the Sagaing fault by the continuous GPS method is more reliable than previous researches.

Since 2011, Myanmar has been established continuous (permanent) GPS network across the Sagaing fault. This GPS network includes two transects and totally, eight continuous (permanent) GPS stations have been operating on this network. The subject of the study is based on the processing of Myanmar continuous (permanent) GPS network for monitoring tectonic movements of the Sagaing fault.

The purpose of this study was to determine the Sagaing fault slip rate from Myanmar cGPS observations by using the GAMIT/GLOBK and to find out the kinematic processing of using the TRACK program. These GAMIT/GLOBK and TRACK programs can perform to get GPS station velocities and relative motion across the Sagaing fault. From the present study, using the GPS observation, the Sagaing fault's tectonic activities can be monitored. This analysis method is useful in many ways to make a research on monitoring the Sagaing fault tectonic actives in Myanmar. Four years of continuous GPS data between 2011 and 2014 were processed in this study.

1.2 Objectives

The aims of this study are to analyze the Myanmar cGPS network observations to get a moving rate of every GPS point by using the GAMIT and GLOBK software and to investigate the post seismic moving rate due to the 2012 Thebeikkyin earthquake by using the TRACK kinematic processing program.

The main points for the present study are:

- Step by step processing the GAMIT, GLOBK and TRACK program.
- Determine the moving rate of the Sagaing fault from each cGPS point.
- Process kinematic positioning during the Thabeikkyin earthquake.

1.3 Scope of Investigation

In this study, Myanmar cGPS network observations, data have been processed and analyzed during 2011 to 2014 by using with GAMIT and GLOBK software. For the

kinematic processing with TRACK program will be focused on 11, November 2012 Thabeikkyin earthquake.

1.4 Expected Contribution

To gain understanding of the more accurate a slip rate of the Sagaing fault and to achieve knowledge of cGPS post-processing and kinematic processing.



CHAPTER 2

THEORY AND LITERATURE REVIEW

This chapter reviews fundamental theories which relate to this study. In section 2.1 presents about the Sagaing fault system. Basic concepts of the GPS are described in Section 2.2 while section 2.3 discusses literature review.

2.1 The Sagaing Fault

Myanmar is composed of two different evolving continents. There are Burma plate and Sunda plate. The Sagaing fault is interpreted as an active dextral strike-slip fault and a continental transform plate boundary that separates the Burma plate and Sunda plate (Curry, Moore et al. 1979, Dain, Tapponnier et al. 1984, Yeats, Sieh et al. 1997, Curry 2005). The Sagaing fault is linked with the Central Andaman spreading center to the south (Curry, Moore et al. 1979). The Andaman Sea was formed by sea floor spreading along short ENE-striking spreading ridges that are offset by NNW-striking transform fault (Curry, Moore et al. 1979). The southern end of the Sagaing fault would be the northernmost part of these transform fault. Extension and rifting in the Central Andaman Basin began at around 11Ma and extension and sea floor spreading has been ongoing since 4-5 Ma (Khan and Chakraborty 2005). That is consequently the best estimate of the age of the Sagaing fault. Spreading in a 335° (N 25° W) direction, relative to present N, is at an average rate of 30mm/yr and the northward component is 27 mm/yr (Curry 2005). The rate of motion of the Burma plate with respect to the Sunda plate motion rate is 18-25 mm/yr towards the north (Socquet, Vigny et al. 2006). The average trend of the Sagaing fault is 351° (N 9° W) and the Sagaing fault accommodates part of the motion while the remainder of the motion is distributed on other faults within a fault zone (Vigny, Socquet et al. 2003). The NW-SE oriented seafloor spreading direction agrees with the average trend of the Sagaing fault. The Sagaing fault is the transform plate boundary with right lateral motion. The NW-SE oriented spreading along ridge segments in the Gulf of Mottama, which are

rifting the Burma Plate northward with respect to the Sunda plate Myanmar region lays in the seismic zone of Alpide-Himalayan Belt. (Aung 2015)

Since Myanmar had experienced many earthquakes in the past which are presumed to be associated with the Sagaing fault, most of historic earthquake records are obtained from the monumental records like old pagodas, temples and stupas because some of the ancient capitals of Myanmar situated along the Sagaing Fault. In the last 100 years, the significant earthquakes occurred in Myanmar are follow: the Ava earthquake of 1839, the Swa earthquake of 1929 (M7.0), the Bago earthquake of 1930 (M7.0), the phyu earthquake of 1930 (M7.0), the Kamaing earthquake of 1931 (M7.6), the Sagaing earthquake of 1956, the Tagaung earthquake of 1946 (M7.3).

The latest large earthquake (M6.8 - Thabeikkyin earthquake, epicenter at 95.883°N, 23.014°E, 9.8 km (depth)) occurred by the Sagaing Fault struck the Thabeikkyin area 100 km north of Mandalay near northern Myanmar cGPS stations in 11, November 2012 (06:30 MST), These research processed kinematic track the effects of that earthquake.

2.2 The GPS Overview

Global Positioning System (GPS) is a space-based satellite navigation system which is designed, financed, deployed and operated by the US Department of Defense (DoD) in the early 1970s. Generally, users can acquire three useful items from the GPS such as Position (Latitude, Longitude and Height), Velocity (Velocity North, East and Up) and Time – (UTC- Universal Time Coordinated)

Moreover, the GPS has some of the useful features that the GPS can be performed better accuracy from meter level reduce to millimeter level, in any weather condition, velocity and time, No inter-station visibility is needed for high precision positioning, results are obtained with reference to a single, global datum, signals are available to users anywhere on earth, free of charge and available day or night. Today, the GPS technology is a useful application for geodetic and mapping as well as in engineering field, environmental, planning, GIS, aircraft and ship location applications.

The basic idea of the GPS is based on a trilateration method to get position by measuring distances to points at coordinates. Trilateration method requires at least three ranges to three known points. The GPS system provides three-dimensional position with a precision of a few millimeters. The satellite constellation was nominally run of 24 satellites, but now currently consists of 32 satellites placed in orbit at the above of 20200km (about three times the earth's radius) over the earth.

2.1.1 GPS for Geodetic Measurements

The GPS have been used for monitoring tectonic activities for the past decade. Nowadays, the GPS can be performed millimeter positioning accuracies due to improvement in the data processing algorithms, hardware of GPS and measurement strategies. One of the techniques is a carrier beat phase technique which can be performed in the most precise geodetic measurement with GPS. This carrier beat phase technique measurements with the post-mission information in the estimation procedure which is also known as precise orbits and satellite clock corrections. A second technique of GPS measurement is the pseudorange. This technique provides the primary GPS observation for navigation, but not sufficient for geodetic surveys.

Continuously operating (permanent) GPS measurement is one of the most popular survey styles for measuring a very small ground motions on faults. Continuous GPS provides continuous position time series with north, east and up (N, E, U) components. The cGPS system is not needed to change the antenna setup over long time periods.

The continuous GPS networks have been used in two kinds of applications. The first is in relation to geodetic objectives such as the measurement of deformation monitoring continuously, and the second is in near real-time, differential GPS services. For monitoring the plate tectonics, it is very important to obtain high precision positioning results from the GPS observations. The GPS technology was not only identified as the best available tool for monitoring of the Sagaing fault, but also can provide the 3-D displacements of the Earth's surface motion. Furthermore, it is considered as an important tool for monitoring of ground deformation caused by seismic activities.

2.1.2 The GPS System

The GPS system consists of four main segments (Blewitt 1997). They are;

1. The space segment, which includes the satellites and transmitted signals.
2. The control segment, which is for the monitoring and operation of the satellite and signals.
3. The user segment, which consists of user equipment and processing software for positioning, navigation, and timing applications.
4. The ground segment, which includes civilian tracking networks of reference stations.

2.1.3 Space Segment

The Space Segment of the system includes of the constellation of the GPS satellites which send radio signals from space. A constellation of GPS satellite is located in six circular orbital planes, which have about 63-degree inclinations to the earth's

equator (shown in Figure 2.1). Three main basic functions of the GPS satellite are: To receive and store data uploaded by control segment, to maintain accurate time by means of onboard atomic clocks, and to transmit information and signal to the user on two L-band frequency.

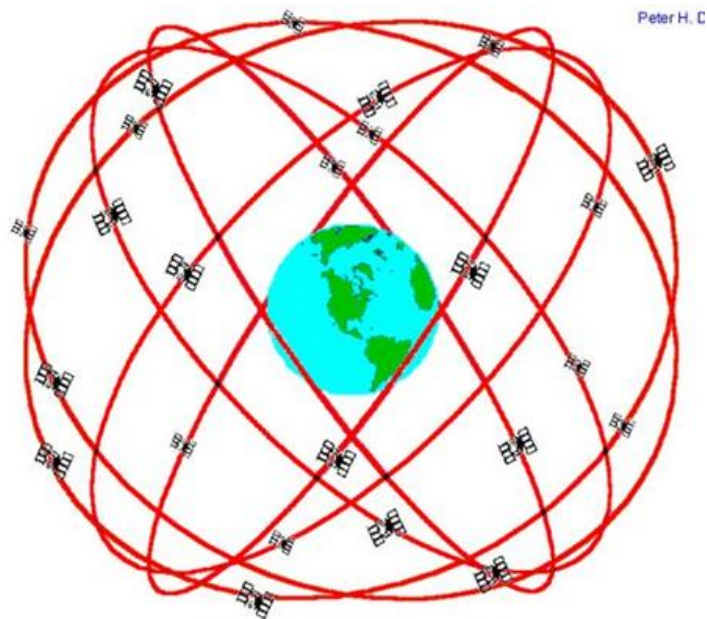


Figure 2.2 The GPS nominal constellation (Dana 2000)

2.1.4 Control Segment

The Control Segment consists of a system of tracking stations located around the world which for satellite health monitoring, telemetry tracking, satellite orbit and clock error computations. There are five ground facilities, stations: Hawaii, Colorado Springs, Ascension Island, Diego Garcia and Kwajalein. The Master Control Station (MCS) is located at Schriever Air Force Base in Colorado. The MCS uploads ephemeris and clock data to the satellite.

2.1.5 User Segment

The User Segment consists of user equipment and processing software for positioning, navigation, and timing applications. The GPS receivers are required to measure for geodetic positioning. Normally, the GPS antenna receives radio signals from the GPS satellites. And then the GPS receiver converted satellite signals into

position, velocity, and time estimates. Four satellites are required to compute the four dimensions of X, Y, Z (position) and Time.

2.1.6 The Ground Segment

The Ground Segment consists of civilian tracking networks that providing the User Segment with real-time Services (DGPS), precise ephemerides and reference control.

2.1.7 The GPS Signals

Each GPS satellite continuously broadcasts ranging codes and navigation on the two carrier frequencies (L1 and L2) to the earth. The satellite atomic clock produces the fundamental frequency, 10.23 MHz. The L1 signal (carrier frequency is generated by multiplying the fundamental frequency by 154, (1575.42) MHz, wavelength of 19.0 cm) is the principal GPS carrier signal and is modulated by the P “precise” code (chipping rate about 10 MHz) which is also known as the Precise Positioning Service (PPS), C/A “course acquisition” code (chipping rate about 1MHz) which is also known as the Standard Positioning Service (SPS) and navigation message. The L2 signal (carrier frequency is generated by multiplying the fundamental frequency by 120, (1227.60) MHz, wavelength of 24.4 cm) is modulated with only P code and navigation message.

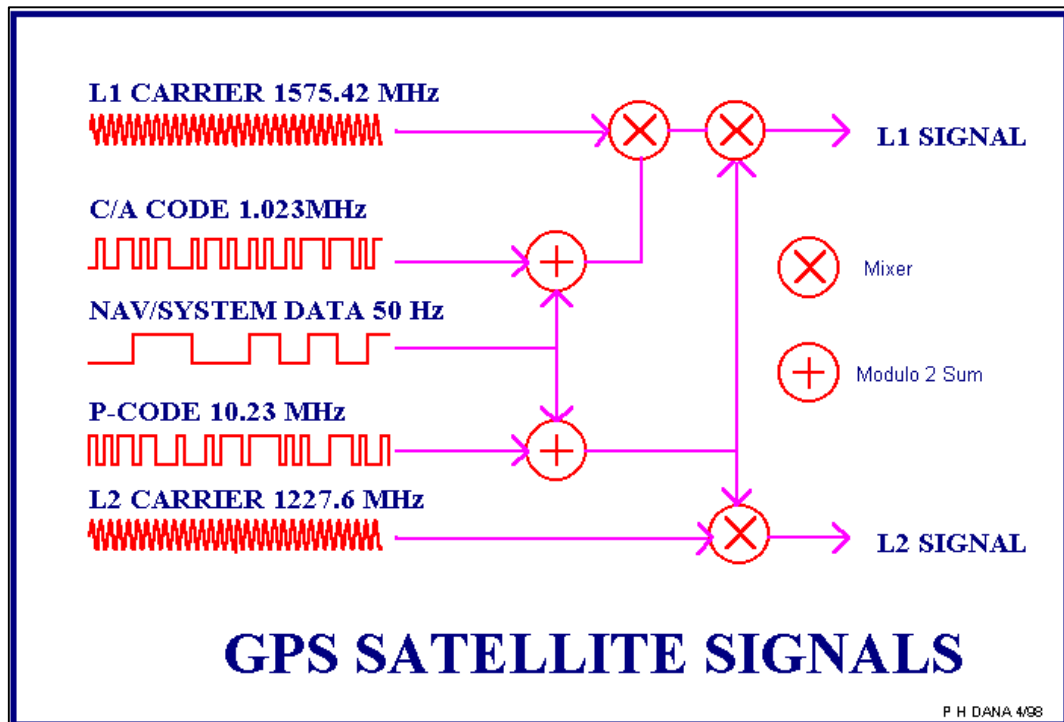


Figure 2.3 The GPS satellite signals (Dana 2000)

2.1.8 The GPS observables

The GPS uses the pseudorange derived from the satellite signal. The pseudorange is derived either from the time difference between a satellite and a GPS antenna and multiplying with speed of light or by measuring the phase of the signal. In both cases, it still includes clock errors because these clocks are never perfectly synchronized and other bias like ionospheric and tropospheric delay, multipath and receiver noise.

$$p = \rho + c \times (dt - dT) + d_{ion} + d_{trop} + \epsilon_p$$

Equation 2-1

Where; p - pseudorange, ρ - geometric range to satellite, c - speed of light, dt and dT - satellite and receiver clock bias, d_{ion} and d_{trop} - the ionospheric and tropospheric delays, ϵ_p - multipath errors and receiver noises.

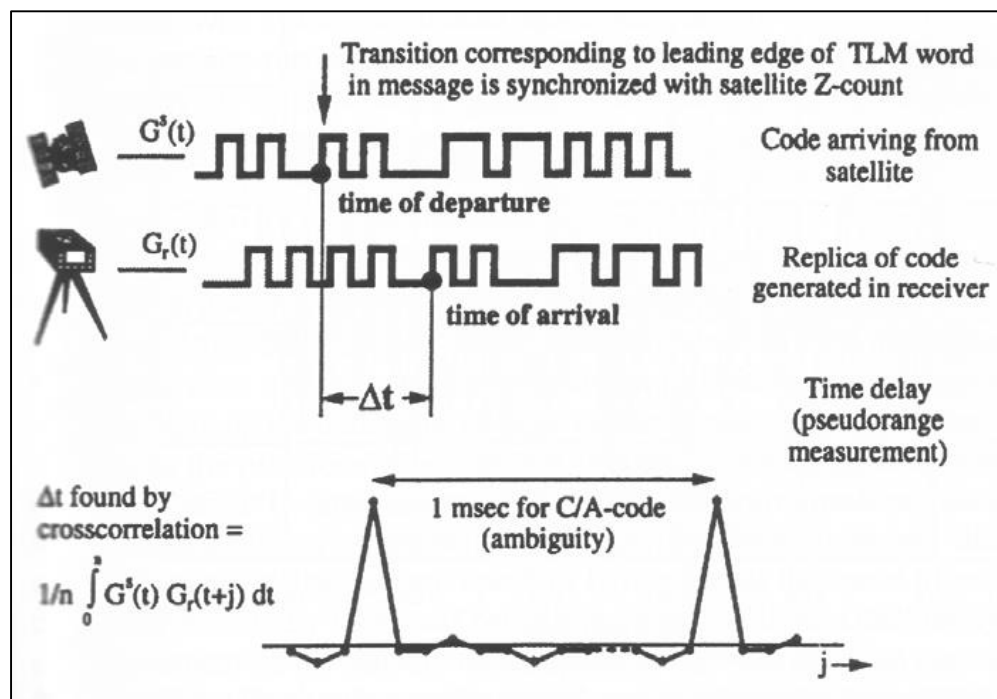


Figure 2.4 measuring the pseudorange (Langley 1997)

The GPS are performed to get the high-precision geodetic results by using the carrier beat phase. It is a more precise observable than the pseudorange. The carrier beat phase could be measured less than centimeter level. The problem of the carrier phase measurement is that the GPS receiver cannot distinguish one cycle of a carrier from another (Blewitt 1997). To get the distance from satellite to GPS receiver multiplies with number of cycle N and the carrier wavelength λ .

$$\phi = \rho + c \times (dt - dT) + \lambda \times N - d_{ion} + d_{trop} + \epsilon_p$$

Equation 2-2

Where; N - integer number of cycles, λ - the carrier wavelength, ρ - pseudorange, $\mathbf{\rho}$ - geometric range to satellite, c - speed of light, dt and dT - satellite and receiver clock bias, d_{ion} and d_{trop} - the ionospheric and tropospheric delays, ϵ_p - multipath error and receiver noise.

2.1.9 Observable in Data Processing

In the GPS measurement, the accuracy of the computed GPS position is affected by errors and biases. The error sources can be classified three main groups. There are satellite-related (Clock bias, orbital errors), receiver-related (Antenna phase

center variation, Clock bias, multipath) and atmospheric errors and biases (Ionospheric refraction, Tropospheric refraction).

A major part of the GPS errors and biases can be removed and reduced by combining their GPS observables. The measurements collected at between GPS receivers or between satellites differences. The errors and biases will be reduced significantly.

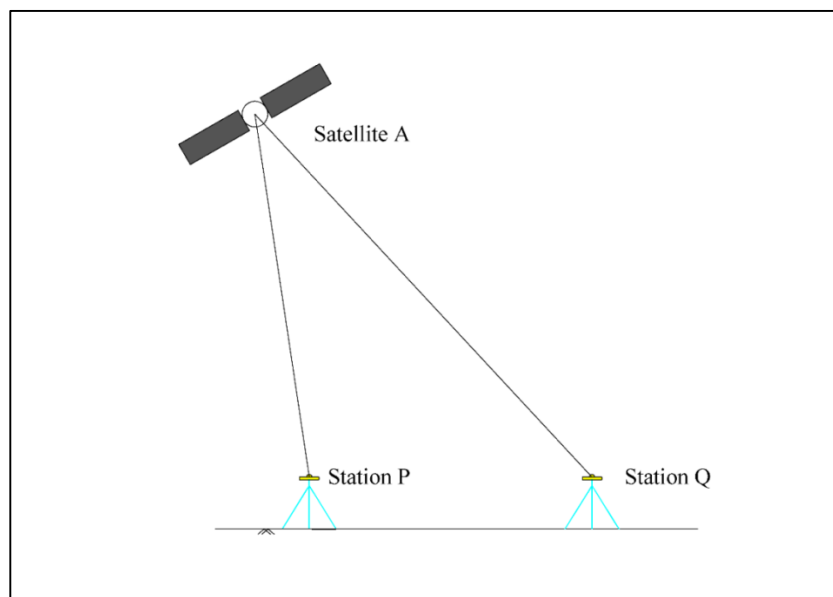


Figure 2.5 Two receivers P and Q observe one satellite A

The between receivers single difference, when two different GPS receivers simultaneously tracking the same satellite can be removed the effect of bias or satellite clock error. If the stations are closely spaced, between receivers single differences technique also reduces the effects of tropospheric and ionospheric delays. P and Q observe same satellite, A (Figure 2.5).

$$\phi_P^A = \rho_P^A - c \times (dt^A - dT_P) + \lambda \times N_P^A - d_{ionP}^A + d_{tropP}^A + \varepsilon_P^A$$

Equation 2-3

$$\phi_Q^A = \rho_Q^A - c \times (dt^A - dT_Q) + \lambda \times N_Q^A - d_{ionQ}^A + d_{tropQ}^A + \varepsilon_Q^A$$

Equation 2-4

The single difference phase is defined as the difference between these two:

$$\Delta\phi_{PQ}^A \equiv \phi_P^A - \phi_Q^A$$

Equation 2-5

$$= (\rho_P^A - c \times (dt^A - dT_P) + \lambda \times N_P^A - d_{ion_P}^A + d_{trop_P}^A + \varepsilon_P^A) -$$

$$(\rho_Q^A - c \times (dt^A - dT_Q) + \lambda \times N_Q^A - d_{ion_Q}^A + d_{trop_Q}^A + \varepsilon_Q^A)$$

Equation 2-6

$$= (\rho_P^A - \rho_Q^A) + c(dT_P - dT_Q) + \lambda(N_P^A - N_Q^A)$$

$$- (d_{ion_P}^A - d_{ion_Q}^A) + (d_{trop_P}^A - d_{trop_Q}^A) + (\varepsilon_P^A - \varepsilon_Q^A)$$

Equation 2-7

$$= \Delta\rho_{PQ}^A + (c \times \Delta dT_{PQ}) + (\lambda \times \Delta N_{PQ}^A) - \Delta d_{ion_{PQ}}^A + \Delta d_{trop_{PQ}}^A$$

$$+ \Delta\varepsilon_{PQ}^A$$

Equation 2-8

Where; Δ - between receivers P and Q, ρ - geometric range to satellite, c - speed of light, dT - receiver clock bias, N and λ - ambiguities term, d_{ion} - the ionospheric delay, d_{trop} - tropospheric delay, ε_p - effect of multipath, observation noise and residual bias.

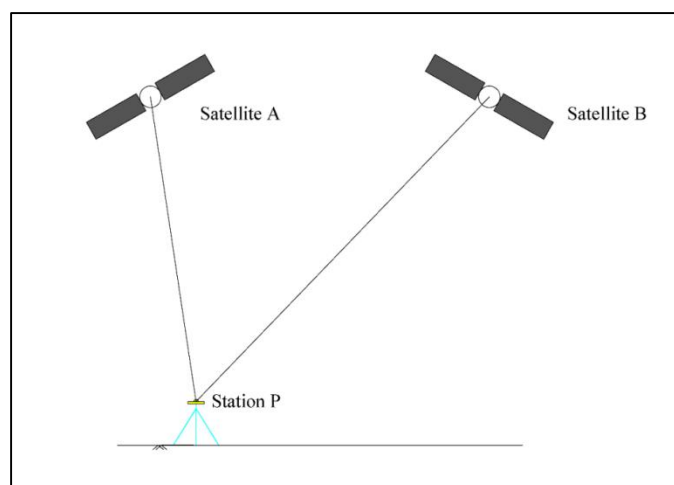


Figure 2.6 One receiver P observe two satellites A and B

The between satellites single difference (When one receiver tracking two satellites) can be removed the receiver clock bias. Receiver, P is observing satellites, A and B (Figure 2.5).

$$\phi_P^A = \rho_P^A - c \times (dt^A - dT_P) + \lambda \times N_P^A - d_{ion_P}^A + d_{trop_P}^A + \varepsilon_P^A$$

Equation 2-9

$$\phi_P^B = \rho_P^B - c \times (dt^B - dT_P) + \lambda \times N_P^B - d_{ion_P}^B + d_{trop_P}^B + \varepsilon_P^B$$

Equation 2-10

The single difference phase is defined as the difference between these two:

$$\Delta\phi_P^{AB} \equiv \phi_P^A - \phi_P^B$$

Equation 2-11

$$= (\rho_P^A - c \times (dt^A - dT_P) + \lambda \times N_P^A - d_{ion_P}^A + d_{trop_P}^A + \varepsilon_P^A) -$$

$$(\rho_P^B - c \times (dt^B - dT_P) + \lambda \times N_P^B - d_{ion_P}^B + d_{trop_P}^B + \varepsilon_P^B)$$

Equation 2-12

$$= (\rho_P^A - \rho_P^B) + c(dt^A - dt^B) + \lambda(N_P^A - N_P^B) - (d_{ion_P}^A -$$

$$d_{ion_P}^B) + (d_{trop_P}^A - d_{trop_P}^B) + (\varepsilon_P^A - \varepsilon_P^B)$$

Equation 2-13

$$= \nabla\rho^{AB} + (c \times \nabla dt^{AB}) + (\lambda \times \nabla N^{AB}) - \nabla d_{ion}^{AB} + \nabla d_{trop}^{AB} +$$

$$\nabla\varepsilon^{AB}$$

Equation 2-14

Where; ∇ - between satellites A and B, ρ - geometric range to satellite, c - speed of light, dt - satellite clock bias, N and λ - ambiguities term, d_{ion} - the ionospheric delay, d_{trop} - tropospheric delay, ε_P - effect of multipath, observation noise and residual bias.

Difference either the between receivers or the between-satellite difference pairs could be formed that so called the double difference. This combination can be

removed both the receiver and satellite clock biases. Two receivers P and Q observing satellites A and B (Figure 2.6)

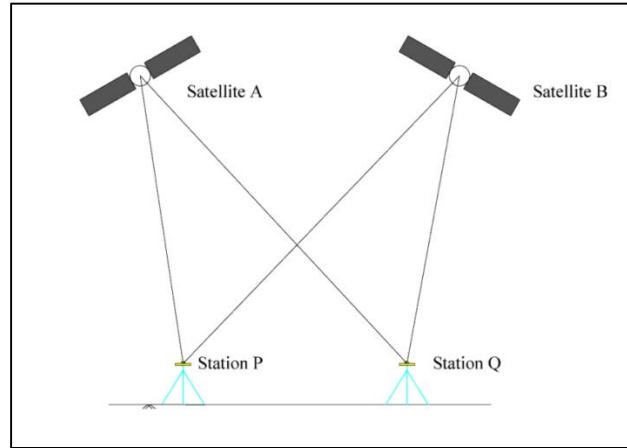


Figure 2.7 Two receivers P and Q observe two satellites A and B

$$\phi_{PQ}^A = \rho_{PQ}^A - c \times (dt^A - dT_{PQ}) + \lambda \times N_{PQ}^A - d_{ionPQ}^A + d_{tropPQ}^A + \varepsilon_{PQ}^A$$

Equation 2-15

$$\phi_{PQ}^B = \rho_{PQ}^B - c \times (dt^B - dT_{PQ}) + \lambda \times N_{PQ}^B - d_{ionPQ}^B + d_{tropPQ}^B + \varepsilon_{PQ}^B$$

Equation 2-16

The double difference phase is defined as the difference between these two.

$$\nabla \Delta \phi_{PQ}^{AB} \equiv \Delta \phi_{PQ}^A - \Delta \phi_{PQ}^B$$

Equation 2-17

$$\begin{aligned} &= \left(\rho_{PQ}^A - c \times (dt^A - dT_{PQ}) + \lambda \times N_{PQ}^A - d_{ionPQ}^A + d_{tropPQ}^A + \varepsilon_{PQ}^A \right) \\ &- \left(\rho_{PQ}^B - c \times (dt^B - dT_{PQ}) + \lambda \times N_{PQ}^B - d_{ionPQ}^B + d_{tropPQ}^B + \varepsilon_{PQ}^B \right) \end{aligned}$$

Equation 2-18

$$= (\rho_{PQ}^A - \rho_{PQ}^B) + \lambda(N_{PQ}^A - N_{PQ}^B) - (d_{ionPQ}^A - d_{ionPQ}^B) + (d_{tropPQ}^A - d_{tropPQ}^B) + (\epsilon_{PQ}^A - \epsilon_{PQ}^B)$$

Equation 2-19

$$= \nabla\Delta\rho_{PQ}^{AB} + (\lambda \times \nabla\Delta N_{PQ}^{AB}) - \nabla\Delta d_{ionPQ}^{AB} + \nabla\Delta d_{tropPQ}^{AB} + \nabla\Delta\epsilon_{PQ}^{AB}$$

Equation 2-20

Where; $\nabla\Delta$ - between satellites (A and B) and between receivers (P and Q), ρ - geometric range to satellite, c - speed of light, N and λ - ambiguities term, d_{ion} - the ionospheric delay, d_{trop} - tropospheric delay, ϵ_p - effect of multipath, observation noise and residual bias.

2.1.10 Linear Combinations of Observations

Some of the useful linear combinations are the ionosphere-free linear combination of carrier phase, the extra wide lane geometry-free linear observation, the wide lane observation and the ionosphere-free and geometry-free combination of carrier phase and code observations (Beutler, Bock et al. 2007, Herring, King et al. 2010).

On short baselines, the ionospheric delays can be reduced with the between receivers single differencing. For baselines longer, vice versa, on which the effect of ionospheric delays are interrelated, it is suitable to form linear combination (LC) and completely removed the ionospheric effect. The linear combination (this LC, also known as L3 or ionosphere-free) of the L1 and L2 phase measurements reduces the ionospheric delay. But a linear combination (LC) forming may magnify other sources of error. [(Bender and Larden 1985), (Bock Y. 1986), (Dong 1989)]

$$\phi_{LC} = \frac{f_{L1}^2}{f_{L1}^2 - f_{L2}^2} \phi_{L1} - \frac{f_{L2}^2}{f_{L1}^2 - f_{L2}^2} \phi_{L2}$$

Equation 2-21

Where; f_{L1} - L1 signal (1,575.42 MHz), f_{L2} – L2 signal (1227.6 MHz). Expressed in units:

$$\phi_{LC} = 2.546\phi_{L1} - 1.984\phi_{L2}$$

Equation 2-22

Another useful combination is geometry free combination (this LG- sometime called L4 or extra wide lane Linear Combination (EX-WL) or geometry-free combination (LG)) which is the difference between L2 and L1. The LG phase is can be lessened the effect of geometrical and the tropospheric delays. The quantity LG combination is independent of the receiver clock as well as of geometry (orbits, station coordinates)

$$\phi_{LG} = \phi_{L2} - \frac{f_{L2}}{f_{L1}} \phi_{L1}$$

Equation 2-23

Expressed in distance units:

$$\phi_{LG} = \phi_{L2} - 0.779\phi_{L1}$$

Equation 2-24

The wide lane (WL) observation (sometimes called L5) mainly used for ambiguity and cycle slip fixing. The WL (L5) is a useful value for ambiguity resolution because it is wide wavelength.

$$WL(L5) = \phi_1 - \phi_2$$

Equation 2-25

The Melbourne-Wubben wide lane combination (MW-WL) (sometimes called L6) is phase and pseudorange combination (L1, L2 and P1, P2) that removes geometry, ionospheric and clock effects. The wide lane (WL) combination observable are able to use for fixing cycle slips (Blewitt 1990).

$$MW - WL = n_1 - n_2 = \phi_1 - \phi_2 - \left(\frac{P_1}{\lambda_1} + \frac{P_2}{\lambda_2} \right) \frac{(f_1 - f_2)}{(f_1 + f_2)}$$

2.1.11 International Terrestrial Reference Frame (ITRF)

Geodetic surveys are commonly needed a global reference frame to compare and combine measurements in different locations, at different times and with different techniques. For this purpose, a terrestrial reference frame provides a set of coordinates any points located on the Earth's surface. GPS data processing is needed a terrestrial reference that can be seen as a two steps process. One is a phase and pseudorange observables which are associated with relative study area and the second is quasi-observations to positions and velocities in a well-defined reference frame. The International Terrestrial Reference Frame (ITRF) is the best global reference frame for all modern geodetic techniques by a set of points with their 3-dimensional Cartesian coordinates. The ITRF is maintained by the International Earth Rotation and Reference Systems Service (IERS) which was created in 1988 to establish and maintain a Celestial Reference Frame (ICRF), in charge of providing global references to the astronomical, geodetic and geophysical communities, promotes the realization of the International Terrestrial Reference System (ITRS). The IERS monitors the Earth Orientation Parameters (EOPs) for the scientific community through a global network of observing stations (Altamimi, Sillard et al. 2002). Nowadays, four main geodetic techniques are used to compute accurate coordinates: the GPS observations, Very Long Baseline Interferometry (VLBI), Satellite Laser Ranging (SLR), and Doppler Orbitography and Radiopositioning Integrated by Satellite (DORIS). The latest version of ITRF is the ITRF2008 which is demonstrated to be of higher quality and more precise than past ITRF solutions. The ITRF2008 estimated an absolute tectonic plate motion model made up of 14 major plates, using velocities of 206 sites of high geodetic quality (Altamimi, Collilieux et al. 2011).

2.1.12 Reference Stations

The International GNSS Service (IGS) is a good constrained solution in the latest version of the ITRF2008. The IGS is a voluntary federation of more than 200 worldwide

agencies that pool resources and permanent GNSS station data to generate precise GNSS products the IGS includes two GNSS (Global Navigation Satellite Systems), GPS and the Russian GLONASS, and intends to incorporate future GNSS. (<http://igsceb.jpl.nasa.gov/>). This allows as the high-precision representation of Myanmar cGPS velocity fields in the international reference frame by constraining the IGS site velocities to their ITRF solution.

2.3 Literature Review

There were already a few researchers that are observed to get the slip rate of the Sagaing fault by using different ways of techniques. First researcher, Curray (1982) found that the slip rate of the Sagaing fault is 35.4 mm/yr. Curray technique is based on spreading of 460 km in 13 Ma through the Andaman Sea spreading center (Curray, Emmel et al. 1982). Myint Thein (1991) research inferred that the Sagaing fault slip rate is half of Curray result, that value is 18.5 mm/yr, assuming a later (11 Ma) initiation of rifting and a 203 km offset of a metamorphic belt near Mandalay (Thein, Tint et al. 1991). Bertrand (1998) calculated the Sagaing fault slip rate from a 2.7-6.5 km offset of a 0.25 to 0.31 million-year old basalt flow in central Myanmar. According their results then indicate a strike-slip velocity, along the fault, situated between 10 ± 1 mm/yr and 23 ± 3 mm/yr that they considered, the whole India-Sundaland relative motion 36 mm/yr is accommodated along the Sagaing fault (Bertrand, Rangin et al. 1998).

Between 1998 and 2000, the campaigns GPS measurements have observed in the central part of the Myanmar near on the city of Mandalay, (Vigny, Socquet et al. 2003). This campaigns GPS network investigated of the present-day crustal deformation along the Sagaing fault. This GPS network included the regional GPS four points and a local GPS 18 sites. Their regional GPS network was located in the rectangle shape of four points (HPAA, LAUN, MIND and TAUN) that design covered to carry out all the deformation between the Main Boundary Thrust on the west side and the Sunda block on the east side, 300 km away. Their local GPS network sites installed at the center in the city of Mandalay across the Sagaing fault. This local GPS network consisted in three transects across the Sagaing fault. Their first campaigns GPS network operated in October 1998.

For their processing, they also used GAMIT and GLOBK software (Herring 1999, King and Bock 1999). As the reference station, they used twelve IGS network stations around their study area (GUAM, IISC, COCO, LHAS, SHAO, KARR, TIDB, TSKB, KUNM, XIAN, WUHN, and YAR1). Their reference frame is ITRF2000 (Altamimi, Sillard et al. 2002). According to their results, the Sagaing/Shan Scarp fault system absorbs lower than 20 mm/yr of the 35 mm/yr India/Sundaland strike-slip motion.

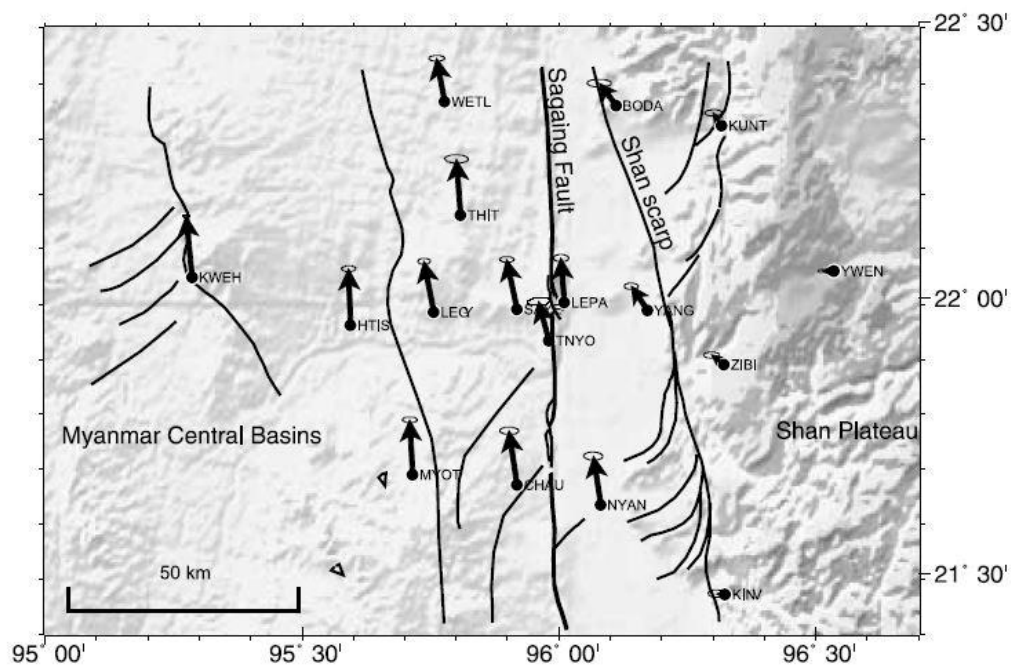


Figure 2.8 Mandalay transects stations (Vigny, Socquet et al. 2003).

The recent research, “Present-day kinematics at the India-Asia collision zone” (Meade 2007) predicted the strike-slip rate between the Indian and Southeast Asian plate is 17 mm/yr and 49 mm/yr at across the central and northern Sagaing fault by means of using GPS observations in the three-dimensional elastic block model for the Indian and Southeast Asian plates. Liu and Bird (2008) estimated a slip-rate of the Sagaing fault of 22-35 mm/yr by using their kinematic model to fit the regional geodetic velocities, geological fault slip rates and stress directions (Liu and Bird 2008). Wang and Sieh measured that the slip rate on the strike-slip Sagaing fault is between 11mm/yr and 18 mm/yr, their field investigations are based on the of the 16th-century fortress wall in southern Myanmar show an offset of ~6 m across the Sagaing fault, the major right-lateral fault between the Sunda and Burma plates. (Wang, Sieh et al. 2011).

According to the finding in the above mentioned researches, the Sagaing fault slip-rate (Thein, Tint et al. 1991, Bertrand, Rangin et al. 1998, Vigny, Socquet et al. 2003, Altamimi, Collilieux et al. 2011, Wang, Sieh et al. 2011) is slower than the slip-rate estimates (Curry, Emmel et al. 1982, Meade 2007, Liu and Bird 2008). In the present study, Myanmar cGPS observations were used to estimate the moving rate of the Sagaing fault.



CHAPTER 3

METHODOLOGY AND DATA PROCESSING

This chapter explains about the methodology of this research and step by step data processing. Section 3.1 is discussing the methodology and presenting flow charts of the research methodology. In section 3.3 presents about the introduction to the Sagaing fault and introduction to Myanmar cGPS network. Section 3.4 shows the equipment of the Myanmar cGPS stations and site monumentation design. Section 3.5 is data collection and preparing step. Section 3.6 is discussing about step by step processing with GAMIT, GLOBK, GGMatlab tool and TRACK programs.

3.1 Methodology

There are two main parts for processing: GAMIT/GLOBK processing section and TRACK processing section. First, the Myanmar cGPS raw data were collected by persons working on the Myanmar Earthquake Committee (MEC). This raw data were converted to RINEX files by using with TEQC program. Not only Myanmar cGPS RINEX files, but also the IGS RINEX files used in processing. And, to obtain the Myanmar cGPS stations coordinates for each day of data in loosely constrained solution (H-files) were used GAMIT software. These H-files are used to sum up solutions for the processing of geodetic data using the GLOBK. To get the time series plots, in this research used two programs such as the Generic Mapping tool (GMT) and GGMatlab program.

Then, the derived post-seismic displacements due to the Thabeikkyin earthquake were used TRACK program. The kinematic processing method is used to get time series of station motions with high rate GPS observations. Figure 3.1 presents a flow chart of the research methodology.

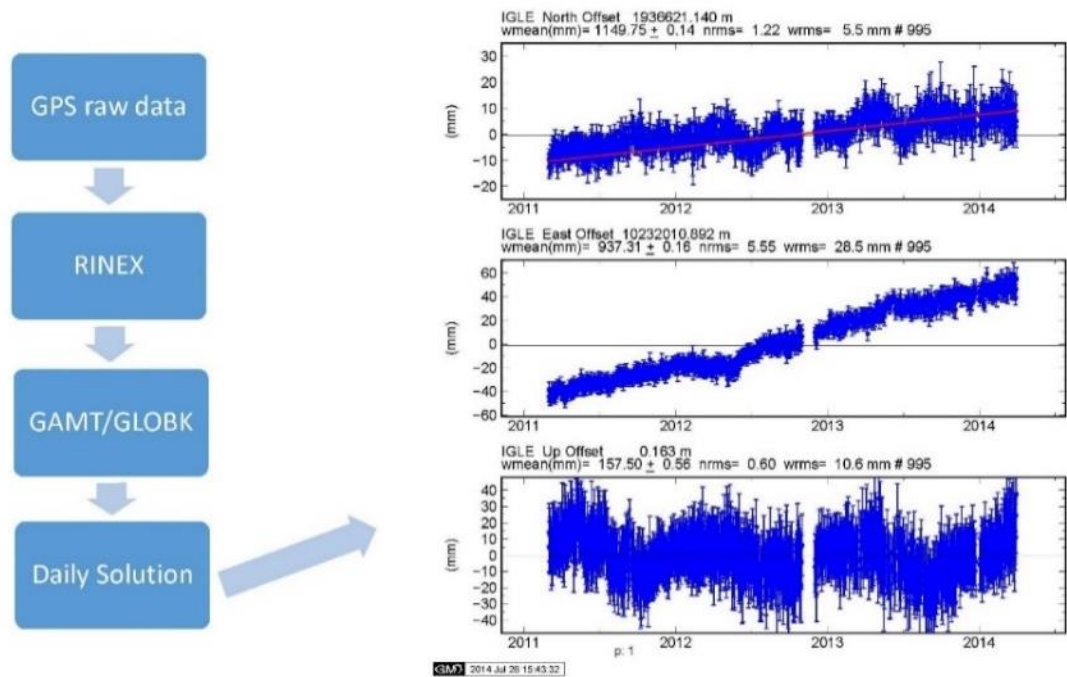


Figure 3.1 Methodological flow chart of GPS data processing (using with GAMIT and GLOBK software).

3.2 Introduction to Myanmar cGPS network

Myanmar cGPS network has established in 2011 jointly organize with Myanmar Earthquake committee (MEC), Earth Observatory of Singapore (EOS) and Department of Meteorology and Hydrology (DMH - Myanmar). This network is used to continuously measure the deformation of the Sagaing fault.

The Myanmar cGPS network includes two cGPS transects. There are northern transect and southern transect. This cGPS network includes eight continuously operating reference stations (CORS). These sites are GYBU, IGLE, WAAW, SATG, HAKA, KANI, SWBO and SDWN. The GYBU, IGLE, WAAW and SATG stations are in southern cGPS transect while the HAKA, KANI, SWBO and SDWN stations are in northern cGPS transect (see Table 3.1 and Figure 3.4). The southern transect has been operating since March 2011, and the northern transect has been operating in February 2012. Totally, Myanmar cGPS network of eight permanent GPS stations has been observing moving rate of the Sagaing fault.

Each Myanmar cGPS network stations are equipped with Trimble GNSS choke ring antennas (Figure 3.2), the Trimble NetR8 and NetR9 receivers (Figure 3.3 and table 3.1) and solar power supply system. This choke ring antenna is proven to reduce the multipath errors. These types of receivers are a multiple frequency GNSS receivers. It can track all GPS (L1, L2, and L5) and GLONASS (L1 and L2) signal. The 24-hour sessions with measurement rate at every 15 seconds, positions 1-minute data rate were observed at all GPS stations. The cut-off angle of the receivers was set to measure the satellites down to 10°.

Table 3-1 List of the Myanmar cGPS stations, Instrument type, coordinates and station to station distance.

Station	Instrument	Latitude	Longitude	Sta. to Sta. Distance
GYBU	Trimble NetR9	17°22'11.66"N	96° 1'33.83"E	0 km
IGLE	Trimble NetR8	17°23'49.06"N	96°19'19.94"E	32 km
WAAW	Trimble NetR8	17°28'9.84"N	96°40'1.84"E	37 km
SATG	Trimble NetR8	17°27'44.74"N	97° 5'48.99"E	46 km
HAKA	Trimble NetR9	22°38'4.15"N	93°36'16.15"E	0 km
KANI	Trimble NetR9	22°26'2.56"N	94°50'47.38"E	129 km
SWBO	Trimble NetR9	22°34'20.59"N	95°43'5.00"E	92 km
SDWN	Trimble NetR9	22°35'11.44"N	96° 7'7.97"E	42 km



Figure 3.2 IGLE GPS station Antenna (Trimble choke ring type antenna)



Figure 3.3 IGLE GPS station receiver box (Trimble NetR8 GNSS receiver)

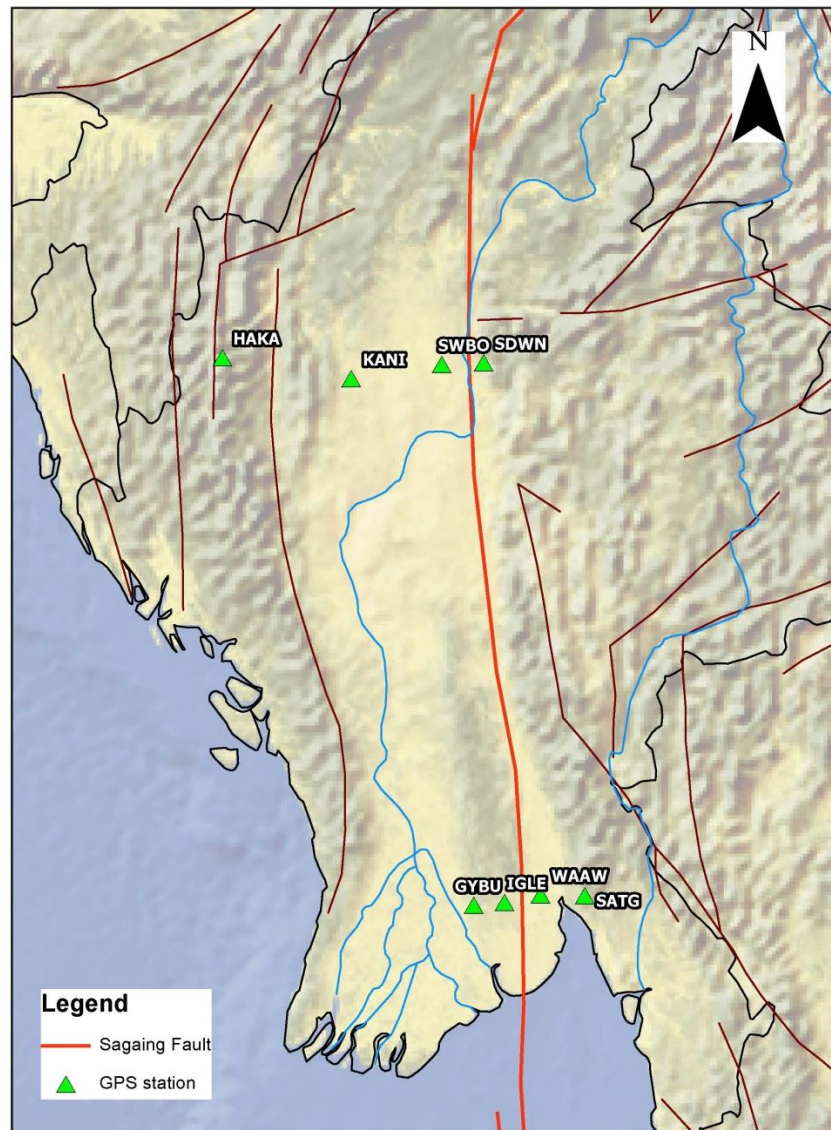


Figure 3.4 Myanmar permanent cGPS stations Location map. HAKA, KANI, SWBO and SDWN are northern transect of Myanmar cGPS network. GYBU, IGLE, WAAW and SATG are southern transect of Myanmar cGPS network.

3.3 Equipment and Site Monumentation

Myanmar cGPS system consists of separate components known as solar power system (two batteries, solar power controller and two solar panels), as it was mentioned before in section 3.3 - the antenna type is Trimble choke ring type GNSS antenna and the receiver (Trimble NetR8 and NetR9). There are a variety of antenna

mounting types over the survey monument. Proper antenna set-up is one of the important things of a continuous GPS survey.

For site monumentation in Myanmar cGPS stations used 3 meter long stainless steel tripods. Centering stainless steel rod is 4 meter long with an adaptor to install the antenna on top of the steel rod. Around 2.7 meter is anchored inside the bedrock (figure – 3.5).

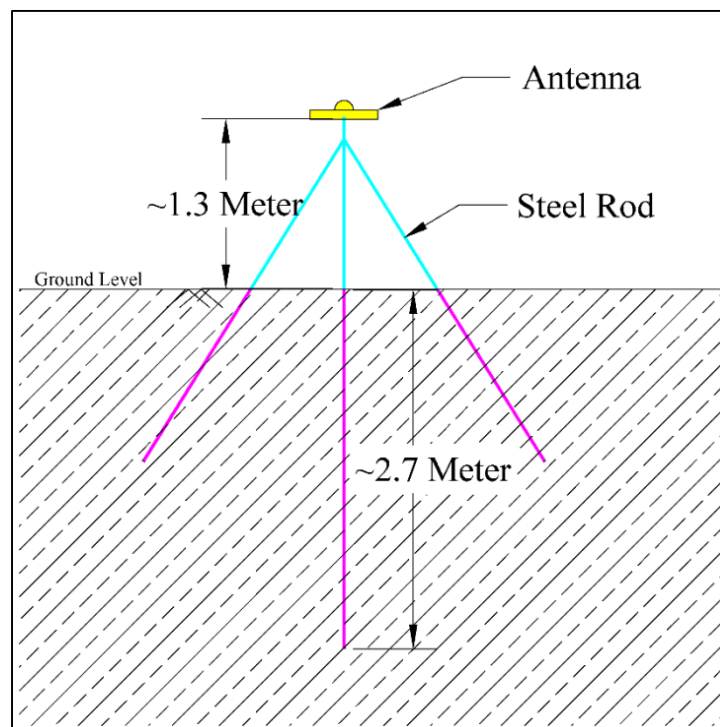


Figure 3.5 Design for monumentation, steel tripod used in Myanmar cGPS network

3.4 Data collection and preparation

The Myanmar cGPS raw data was kindly provided by Myanmar Earthquake Committee (MEC). Data from both of the cGPS transects measurements from 2011 was stored in the MEC data center. Every three months, MEC's staff would be collecting all of the GPS data by using manual download method. The Trimble GNSS receivers were used for the measurement of the local cGPS stations. Myanmar cGPS station receivers are configured with three types of continuous data logging setting. For example, measurement rate of 15 second with 1-minute positioning rate, measurement rate of 1 second with 0.1-second positioning rate and measurement rate

of 0.02 second with 0.1-second positioning rate. For time series, analysis processing were used 15 second with 1-minute positioning measurement rate. For kinematic processing, high rate GPS data (0.02 second with a 0.1-second positioning rate) were used in this study.

In this research, all available cGPS data were used for starting of every station up to March 2014 (see Table 3.2). For the entire survey period, several data gaps occurred at all CGPS stations and they are due to power supply and technical problems. As the time span as shown in Table 3.2 represents 590 days for GYBU, 1072 days for IGLE, 1073 days for WAAW, 592 days for SATG, 732 days for HAKA, 498 days for KANI, 413 days for SWBO and 725 days for SDWN.

And all of the GPS data was stored in the receiver with the Trimble binary format. Thus, it has to convert the Trimble binary format to a receiver independent exchange (RINEX) format using the TEQC software that is the multi-purpose toolkit for GPS/GLONASS data developed by UNAVCO (Estey and Meertens 1999). At this conversion stage, the observation data in RINEX format is planned for the GAMIT processing.

In addition, all local cGPS data and 13 IGS (International GNSS Service) reference stations data are incorporated in the processing step. The IGS stations were used in processing that are BAKO, COCO, CUSV, DARW, DGAR, IISC, KUNM, LHAZ, NTUS, PERT, PIMO, TCMS and XIAN (Figure 3.6).

Table 3-2 Myanmar cGPS stations observation data set used in this research

	2011	2012	2013	2014
GYBU				
IGLE				
WAAW				
SATG				
HAKA				
KANI				
SWBO				
SDWN				



Figure 3.6 Map of the IGS stations which have been used in the Myanmar cGPS network processing

3.5 Data Processing

In this section 3.6 presents about step by step processing with GAMIT and GLOBK software and kinematic processing step. For the entire example processing steps used 2014, day 1 observations data.

3.5.1 Overview of GAMIT Processing

The GAMIT and GLOBK 10.5 (Herring, King et al. 2010) software package has been used for the estimation of three-dimensional relative positions of ground stations coordinates and orbits of GPS satellites from the GPS observations. The GAMIT software is also known as a double differencing approach in a multi-station solution, that it developed at MIT and Scripps.

The primary output of GAMIT is a loosely constrained solution (H-file) of parameter estimates and covariance that can be passed to the GLOBK for combinations of data to estimate station positions, velocities, orbital and Earth rotation parameters. The software is designed to run under any UNIX/LINUX operating system supporting X- Windows. It is associated with several shell scripts which control automatic processing. GAMIT program solves a least squares algorithm to estimate the relative positions of a set of stations, orbital and Earth-rotation parameters, zenith delays, and phase ambiguities by fitting to doubly differenced phase observations.

3.5.2 GAMIT processing

For GPS processing with the GAMIT, the GPS range and phase data, usually for 24 hour sessions of data are needed which collects data from multiple GPS satellites. To obtain the most accurate processing results, some information is needed such as atmospheric models, ocean tides, antenna, receiver biases, the orbits of the satellites information and information about clocks in the satellites. In GAMIT, only crude clock information needed because GAMIT uses the double differencing technique.

In this research, processing type is used the automatic processing type by using with script `sh_gamit` that it is taken from RINEX data over several days to a complete

solution. The first step of the GAMIT processing is to create working directories. Other necessary directories will be automatically created from GAMIT software (See Figure 3.7 for 2014 working directories).

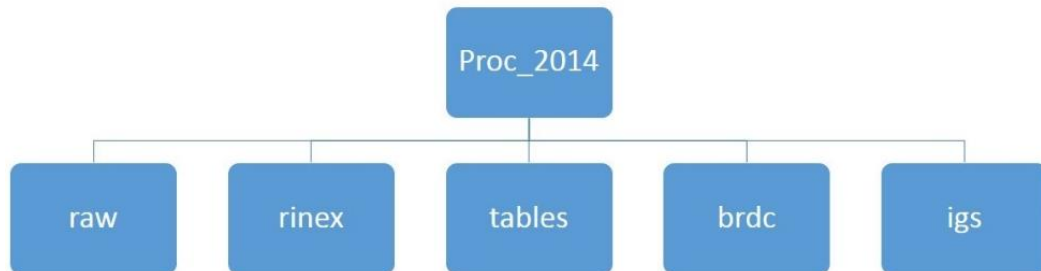


Figure 3.7 Directories structure, create working directories before processing

As the second step, before the processing with GAMIT, the important files prepared and edited in the tables directory: There are:

- RINEX files – Receiver INdependent EXchange format for GPS data
- process.defaults,
- sites.defaults,
- lfile,
- session.info,
- station.info,
- sittbl.,
- sestbl.,
- SP3 or G-file from SOPAC,

And optionally links to the tables: nutabl., Soltab., Luntab, gdetic.dat, leap.sec, svnav.dat, tform.dat, antmod.dat, ut1. and Pole. After prepared the require control files, process.defaults, sites.defaults, session.info, station.info, sittbl. and sestbl. were placed in the tables directory. In this chapter will be discussed about some edited files.

RINEX files: The GAMIT processes GPS phase and range data files by means of RINEX format. Before converting the RINEX files from the local cGPS raw data are

Trimble raw binary data. These raw data were converted to RINEX by using two commands. They are:

- runpkr00 command (convert t00, t02 Trimble raw data to dat file). It would produce dat file.
- teqc command would convert dat file to RINEX file.

In this research, all of the local cGPS data were converted to RINEX by using with these two commands. In addition to the IGS stations data (RINEX files) that is distributed around study area, were downloaded from CDDIS of the NASA archive of space geodesy data. To get the IGS data (RINEX files) uses `sh_get_rinex` command. For example:

```
$sh_get_rinex -archive cddis -yr 2014 -doy 001 -ndays 2 -sites bako coco cusv
darw dgar iisc kunm lhaz ntus pert pimo tcms xian
```

This script will get the data from CDDIS ftp server for specific IGS RINEX data. The IGS RINEX files and local GPS RINEX files are needed to put together to the `rinex` working directory.

process.defaults: is processing control file that contains computation environment, sources for internal and external data and orbit files, for starting time, sampling interval, and instructions for archiving the results. In this research, start time is 0 hr 0 min because of 24 hr session. Sampling interval is 30.

station.info: is station information file. All of the receiver and antenna type, height of instrument (HI) values and other site information are recorded in `station.info` file. This file had to be created by manual editing.

sestbl. and sittbl.: are session control table and site control table. `sestbl.` file containing the GAMIT analysis command and `sittbl.` file specifying a priori constraints for coordinates and station specific models.

The same `sestbl.` file was used for processing of all the sessions separately.

Session Table

Processing Agency = MIT

Satellite Constraint = Y ; Y/N (next two lines are free-format but 'all' must be present)

```

all   a   e   i   n   w   M   rad1 rad2 rad3 rad4 rad5 rad6 rad7 rad8 rad9;
      0.01 0.01 0.01 0.01 0.01 0.01 0.01 0.01 0.01 0.01 0.01 0.01 0.01 0.01

```

Choice of Experiment = BASELINE ; BASELINE/RELAX./ORBIT

Type of Analysis = 1-ITER ; 1-ITER(autcln prefit and conditional redo) / 0-ITER (no postfit autcln) / PREFIT

AUTCLN redo = Y ; Y/N; 3rd soln only if needed, assume 'Y' if 'Type of analysis = 1-ITER'

Choice of Observable = LC_AUTCLN ; LC_AUTCLN (default), LC_HELP (codeless L2), L1_ONLY (L1 soln from dual freq),

```

L2_ONLY (L2 soln from dual freq), L1,L2_INDEPENDENT (L1 + L2 from dual freq)
L1&L2 (same as L1,L2_INDEPENDENT but with ion constraint);
L1_RECEIVER (must add 'L1only' in autcln.cmd)

```

Station Error = ELEVATION 10 5 ; 1-way L1, $a^{**2} + (b^{**2})/(\sin(\text{elev})^{**2})$ in mm. default = 10. 0.

AUTCLN reweight = Y ; Y/N; reweight data from autcln rms; replaces 'Use N-file' in releases < 10.32

AUTCLN Command File = autcln.cmd ; Filename; default none (use default options)

Decimation Factor = 4 ; FOR SOLVE, default = 1

Quick-pre decimation factor = 10 ; 1st iter or autcln pre, default same as Decimation Factor

Quick-pre observable = LC_ONLY ; for 1st soln, default same as Choice of observable

Ionospheric Constraints = 0.0 mm + 8.00 ppm

Ambiguity resolution WL = 0.15 0.15 1000. 99. 15000. ; for LC_HELP, ignored for LC_AUTCLN

Ambiguity resolution NL = 0.15 0.15 1000. 99. 15000. ; allow long baselines with LC_AUTCLN

Zenith Delay Estimation = Y ; Yes/No (default No)

Interval zen = 2 ; 2 hrs = 13 knots/day (default is 1 ZD per day)

Zenith Constraints = 0.50 ; zenith-delay a priori constraint in meters (default 0.5)

Zenith Variation = 0.02 100. ; zenith-delay variation, tau in meters/sqrt(hr), hrs (default .02 100.)

Elevation Cutoff = 10 ; default 0 to use value in autcln.cmd

Atmospheric gradients = Y ; Yes/Np (default No)

Number gradients = 2 ; number of gradient parameters per day (NS or ES); default 1

Gradient Constraints = 0.01 ; gradient at 10 deg elevation in meters; default 0.03 m

For more addition controls detail are showed in appendix section.

The processing could be more efficient with a 1-ITER option for the Type of Analysis control, because the Myanmar cGPS network is sufficiently large to improve the orbit. With this command, there will an additional sequence of MODEL, AUTCLN, SOLVE, and (optionally) ARC to improve the coordinates (and possibly orbit) prior to the final solution. For choice of observable, which used LC_AUTCLN option that is Ambiguity-free and ambiguity-fixed solutions with linear combination (LC).

SP3 precise ephemeris or G-file: The G-file is a file of orbital initial conditions for all satellites on the tabular ephemeris (T-) file which includes satellite state vectors at equally-spaced intervals default for all satellites in a session or series of sessions for later interpolation in the model. To get the T-file for processing was downloaded from Scripps Orbit and Permanent Array Center (SOPAC) analysis center.

3.5.3 Automatic Batch Processing with GAMIT

The next processing step is using automatic batch processing with scripts `sh_gamit`. The `sh_gamit` is taken from RINEX data over a range of days to a complete solution. The following programs are run by the script `sh_gamit` internal operation:

- `makexp` and `makex` prepare the data.
- `fixdrv` prepares the batch control files.
- `arc` integrates GPS satellite orbits.
- `model` calculates theoretical (modeled) phase and partial derivatives of phase with respect to parameters.
- `autcln` repairs cycle slips, removes phase outliers, and resolves the wide-lane ambiguities.
- `solve` estimates parameters via least squares, resolving the narrow-lane ambiguities and creating an H-file for GLOBK.

For example, the complete data set for the 2014, day 1 were processed using a single line.

```
$sh_gamit -d 2014 001-expt myan -orbit IGSF -expt myan
```

For more addition options detail for automatic batch processing with script `sh_gamit` are shown in appendix section.

After finishing the `sh_gamit` command, the initial files which are needed for processing with the GAMIT software, are automatically provided or created in their processing directories. They are:

- Satellite orbits,

- IGS sp3-files (tabular) and/or g-files,
- ARC integrates to get t-files (tabular),
- Earth Orientation Parameters (ut1., wob.),
- Leap second file that allows conversion from GPS time to UTC,
- Satellite clock (j-) files – from RINEX navigation (brdc) file,
- Rcvr/ant characteristics (rcvant.dat, hi.dat),
- Differential code biases (dcb.dat)—update ~monthly,
- Antenna phase center models (antmod.dat),
- Luni-solar ephemerides and nutation (soltab., luntab., nutabl.),
- Ocean tide grid (optional),
- Atmospheric loading grid (optional) and
- Mapping function grid (optional).

GAMIT gives two solutions. The first is coordinated and the second is the final estimates. In this research, the GAMIT final output are the solution Q-file which contains a record of the analysis, auto clean summary file (autcln.sum), an associated covariance matrix ("quasi-observations") of station positions and parameter adjustments for the solution generated with loose constraints H-file, used as input to GLOBK.

To show the example of GAMIT output files is used, data set for the 2014, day 1 file. (For more output Q and H files for 2014, day 1 file details are shown in appendix section). The Q-file gives the estimates of all of the geodetic parameters from a linear combination (LC) solution.

3.5.4 Evaluating of the results

In this study, the main of daily solutions were determined with the data fit the model to their noise level. This criterion is the normalized root mean square (nrms) of the solution. A appropriate solution produces nrms of about 0.25 (King and Bock 1999). In the present study, not over the postfit nrms, values are around 0.2 that mean the solution is acceptable.

3.5.5 Overview of the GLOBK Processing

GLOBK which is a smoothing Kalman filter is a suite of programs designed to combine the results together from the processing of primary data from space-geodetic or terrestrial observations (Herring, King et al. 2010). The primary input of the GLOBK is the quasi-observation files called binary H-files which contain geodetic solutions with loosely constrained full covariance information from the GAMIT processing of GPS data.

There are three common applications in which the GLOBK is used: the first common application is a combination of individual sessions of observations to get a time series of station coordinates. The second application is a combination of individual sessions of observations to obtain an estimate of station coordinates averaged over a multi-day experiment. The third application combines averaged positions to estimate station velocities from several years of observations.

Note for GLOBK that, the GLOBK can be able to assume a linear model. The GLOBK cannot correct deficiencies of the initial loosely constraint solution (H-file). GLOBK can only combine in local H-files with SOPAC global loosely constrained solution from the IGS network stations H-files.

3.5.6 Preparing the input files for The GLOBK

The GLOBK analysis of GPS data has the following structure. The first step for GLOBK processing is collecting the quasi-observation files from GAMIT and global quasi-observation files into the glbf directory. The ASCII quasi observation files or solution files are created from the output of the GAMIT process. The second step is

downloading the continuous global quasi-observation files which are provided by the Scripps Orbital and Permanent Array Center (SOPAC) at the University of California (Bock et al., 1997). To get the global H-files used script `sh_get_hfiles`. For example, command is:

```
$sh_get_hfiles -yr 2014 -doy 001 -net igsall
```

The next step is converting step which is converting the ASCII quasi observation files or solution files into binary H-files. The binary H-files in `glbf` directory can be converted by using with script `htoglb`. The script `htoglb` converts the experiment ASCII solution H-files from the GAMIT into GLOBK binary H-files. For example, for year 2014 day 1 command is:

```
htoglb . ../tables/svs_myexp.svs ../001/hmyana.14001
```

After finishing the converting with script `htoglb`, will generate two different binary files. There are `glr` and `glx` that for biases free and biases fixed loose constrained solutions.

And the next GLOBK processing step is creating the input global file list (*.gdl) in `gsoln` directory. To obtain the `.gdl` list for the biases-fixed H-files created following `.gdl` file. In this `.gdl` file contained additional parameters following the igs global H-files and the experiment H-files name to indicate reweighting and coupling. For example `.gdl` file (with weight 1) is:

```
../glbf/h9609061159_igs1.glr 1.0 +
```

Next processing step is running `glred/glgorg` for all the (binary) H-files from continuous observations to obtain a time series of station coordinates. For example is

```
$glred 6 myan2014.prt myan2014.log myan2014.gdl globk.cmd
```

There are three types of output produced in running this `glred` command. The "log" file that contains a log of the run as each new h-file is added. A loose solution, recorded in `myan2014.prt` "prt". The "org" `glorg` solution file which is the tight constrains solution in the reference frame defined by the `glorg` run. Example output file are shown in Appendix section. To obtain the time series plot results used two plots generate tools. There are Generic Mapping Tool (GMT) and GGMatlab. The GMT program presents in workstation to make the plots using GAMIT/GLOBK scripts. For example commands is

```
$sh_globk_scatter -file myan2014.org
```

Where, the script `sh_globk_scatter` generated two postscript frames, `ps1.myan2014` and `ps2.myan2014`, showing the weighted root mean square (rms) and normalized root mean square (nrms), respectively, versus length. And also created files with the estimates for each station coordinate (VAL.*) and baseline component (val.*), the station coordinate (VAL.*) are extracted into mb.* files by the program `multibase`.

Example is:

```
$multibase VAL.* -d
```

```
$sh_baseline -n 3 -f mb*
```

The script `sh_baseline` created the time series plots. In this thesis, all of the processing results are presented in chapter 4. Each of GPS results with time series plots are generated by using with the generic mapping tool (GMT). To compare the moving rate of the GPS stations results from side by side of the Sagaing fault appended in one plot and to obtain actual yearly moving rate result which removed the post seismic motion due to the earthquake, was used GGMatlab tool.

3.5.7 Overview of the GGMatlab

The GGMatlab tool (Herring 2003) was used for data editing and estimation of station velocities. This tool can provide the quality of the results being obtained from GLOBK analyses of GPS data. The primary aim of the GGMatlab tool is to improve the quality and understanding of the results from large GPS analysis

A time series are often associated with geophysical effects. There are offsets due to earthquakes, post-seismic, and the effects of groundwater changes. The main objective of an outlier editing step is the removal of erroneous samples in order to obtain reliable estimated station velocities. The tools are documented and available from <http://www-gpsg.mit.edu/~tah/GGMatlab>.

One of the parts of GGMatlab tool is 'Tsview' which allows an interactive viewing and manipulation of GPS velocities and time series with a Matlab-based graphical user interface (GUI) (Herring 2003). The main objective of Tsview is to assess the quality of time series and control files. The Tsview will delete bad site position

estimates and account for jumps in time series. In this research, the main reason to use the Tsview, is to compare the moving rates of the GPS station in time series, and to assess the motions of the earthquake. There are two options in Tsview, append and break. To combine the time series of the wet side stations of the Sagaing fault, the tool called append has been used. Likewise, the time series of the east side has been combined. Later the movement of the Thabeikkyin earthquake has been omitted and breaking the moving rate from the annual movement, to find the result which are shown in detail with figures in chapter 4.

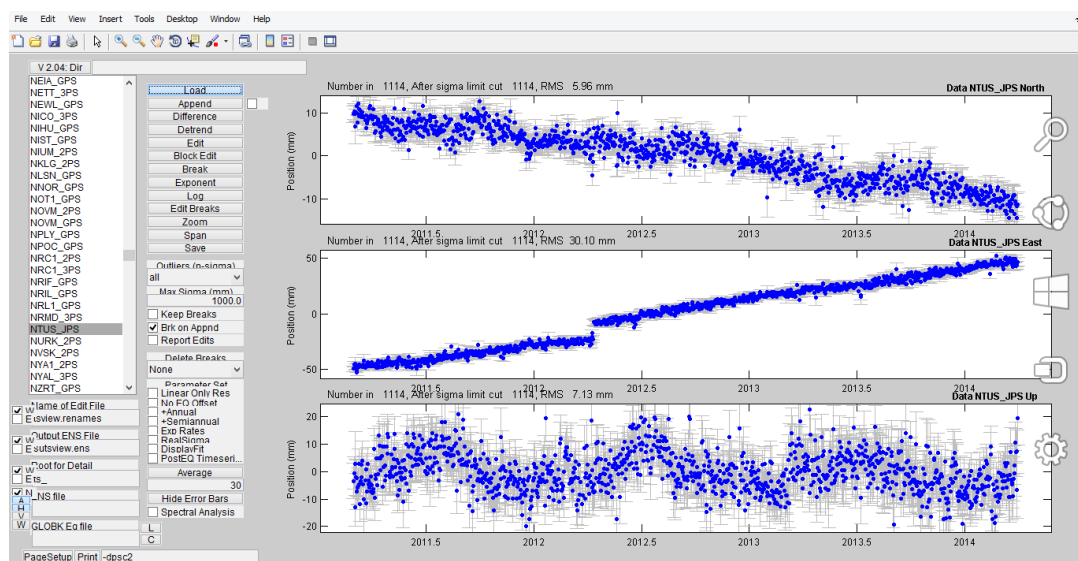


Figure 3.8 Example of a tsviews screen image.

3.5.8 Kinematic Track Processing

The TRACK comprehensive suite of programs (kinematic GPS processing program) is the Massachusetts Institute of Technology (MIT) implementation of this style of processing. Program TRACK uses RINEX data files and SP3 GPS orbit files, but the GAMIT needs a full suite of additional files because TRACK can use some of GAMIT files.

The main purpose for using TRACK program in this research is to obtain seismic motion rate due to the Thabeikkyin earthquake (11, November 2012). The magnitude 6.8 earthquake was occurred the near SWBO and SDWN stations about 50 km away (figure-3.6). Before the TRACK processing, needs preparing the high rate observation

file. In this processing was used 0.02 second with 0.1 second positioning rate observations data.

The basic inputs for TRACK processing are observation files (RINEX), sp3 file. In this processing was used high rate observation RINEX data SWBO and SDWN for 11, November 2012 and LHAZ which is the IGS reference station near the SWBO and SDWN stations.

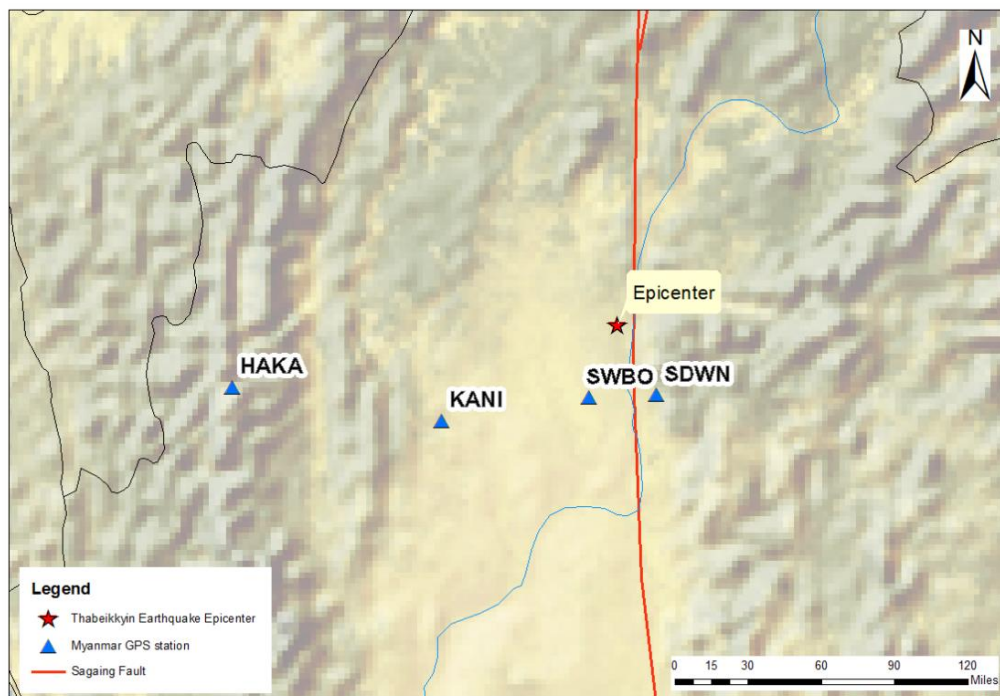


Figure 3.9 Epicenter location map of the M 6.8 Thabeikkyin Earthquake in Myanmar (23.005°N 95.885°E)

The next step is to prepare the TRACK command file (track.cmd). To fill up the RINEX file names correctly. In this case LHAZ IGS station has to be fixed. Using kinematic processing with TRACK, SWBO and SDWN stations are to be processed. Processing day and date have to be included in sp3 file. Therefore 2012 Nov, 11, sp3 name is igs17140.sp3. To get the sp3 file used following command.

```
$sh_get_orbits -archive sopac -yr 2012 -doy 316
```

Where `-yr 2012 -doy316` requests day of year number 316 in the year 2012 that just this one day of data is downloaded. The next step is the position of the sites. The value of coordinate has been copied down from RINEX file. There are three types to calculate the TRACK program. Those are AIR, SHORT and LONG. Air is assumed to

be high-sample rate aircraft. SHORT is Short baseline static data lower than one kilometer baseline. LONG is Long baseline static data greater than one km. In that case, used LONG mode had been used because our stations have long baselines. Sampling intervals kept one second. The output type is kept by NEU in order to attain in a form of North, East and Up (NEU) components. The details of the TRACK command file are shown in an appendix section (E).



CHAPTER 4

RESULTS AND DISCUSSION

After processing the GPS observations, using the methodology, chapter 3 has been described. In section 4.1 presents about Myanmar cGPS Network time series analysis results. Comparing the GPS stations results and discussion are described in section 4.2. In section 4.3 presents about measuring displacement due to the Thabeikkyin Earthquake. Velocity vector map and results are shown in section 4.4. In section 4.5 shows about kinematic processing results and discussion.

4.1. Myanmar cGPS Network Time series results and Discussion

The GPS measures the rate of movement in the north, east and up component that are combined to give information about the location in 3D space. These motions are recorded onto three separate graphs. According to the time series graph, all the stations had similarity in changing of position. The processing of the Myanmar cGPS network initial results obtained from the southern and northern cGPS transects shown in the time series graph of each station's in North, East and Up (N, E, U) components.

As it was mentioned before that the Sagaing fault is a right lateral strike-slip fault system (Curry, Moore et al. 1979). Therefore, the east sides of the fault stations are moving to the south and other sides of the stations are moving to the north. The GYBU and IGLE stations are moving to the northward, the north offset rates imply that about 13.12 ± 0.20 mm/yr and 4.51 ± 0.09 mm/yr respectively. According to the result, the GYBU station moving rate is faster than the IGLE station (see in figure 4.1 and 4.2). And also the WAAW and SATG stations (north offset) moving rates are -6.92 ± 0.09 mm/yr and -8.72 ± 0.15 mm/yr. These two stations are moving to the southward direction with nearly the same velocity (see in figure 4.3 and 4.4). For all stations of the southern transect of the east offset moving rate are nearly same velocities about 30-31 mm/yr.

The HAKA, KANI and SWBO stations, which are the west side of the Sagaing fault, are moving to the northward, the moving rate of 21.50 ± 0.15 mm/yr, 17.89 ± 0.13 mm/yr and 50.42 ± 1.70 mm/yr respectively (see in 4.5, 4.6 and 4.7). The SDWN station

is the east side of the fault, moving rate of -129 ± 2.77 mm/yr (figure 4.8). The HAKA and KANI stations results are normal moving rates, but the SWBO and SDWN stations moving rates are higher than the other two stations because this displacement affected by the 2012 November Thebeikkyin Earthquake. For the east offset moving rate, the HAKA and KANI stations moving rates are between 27-30 mm/yr. The larger error bars in the time series graph of vertical position show the larger errors included in determining vertical location. This study was concentrated on horizontal motions.

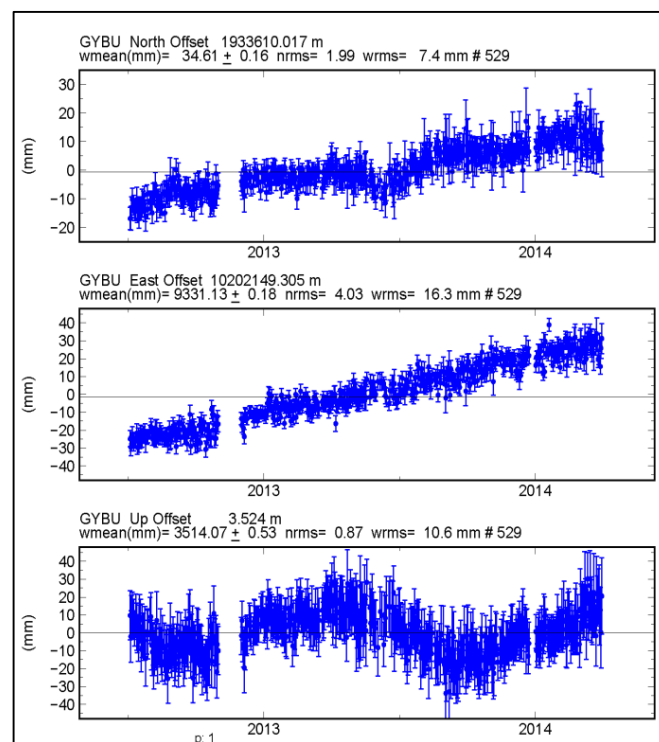


Figure 4.1 Time series of the Myanmar continuous GPS station (GYBU)

Time series of the GYBU station is plotted from top to bottom with north, east and up coordinate components. The time series graph of the GYBU station movement shows the station in northern transect of Myanmar cGPS network that is being pushed back toward the northeast (figure 4.1).

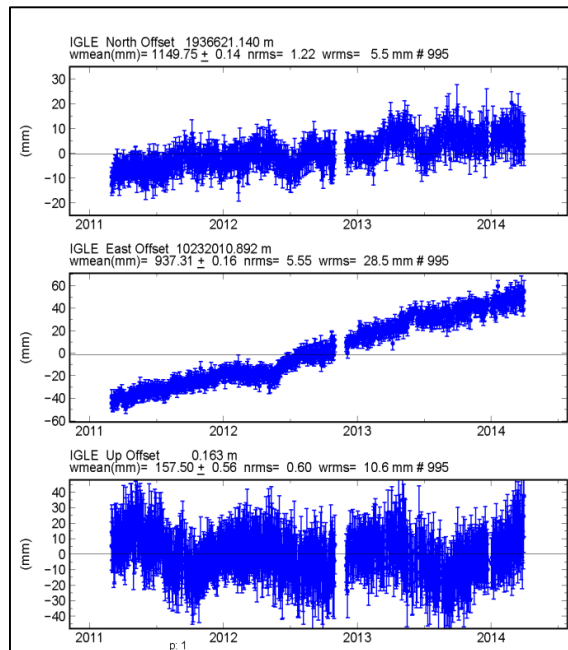


Figure 4.2 Time series of the Myanmar continuous GPS station (IGLE)

Four years' time series of the IGLE is plotted from top to bottom with north, east and up coordinate components. The IGLE station movement illustrates that it is being pushed back toward the northeast (figure 4.2).

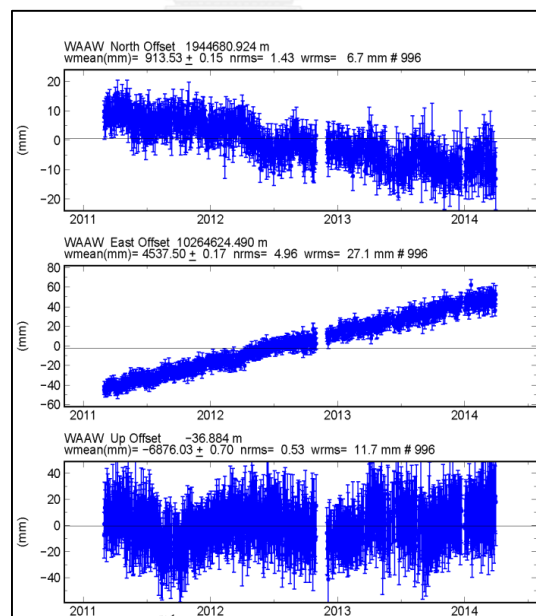


Figure 4.3 Time series of the Myanmar continuous GPS station (WAAW)

The GPS time series of the WAAW is plotted from top to bottom with north, east and up coordinate components. The WAAW station movement proves that it is being pushed back toward the southeast (figure 4.3).

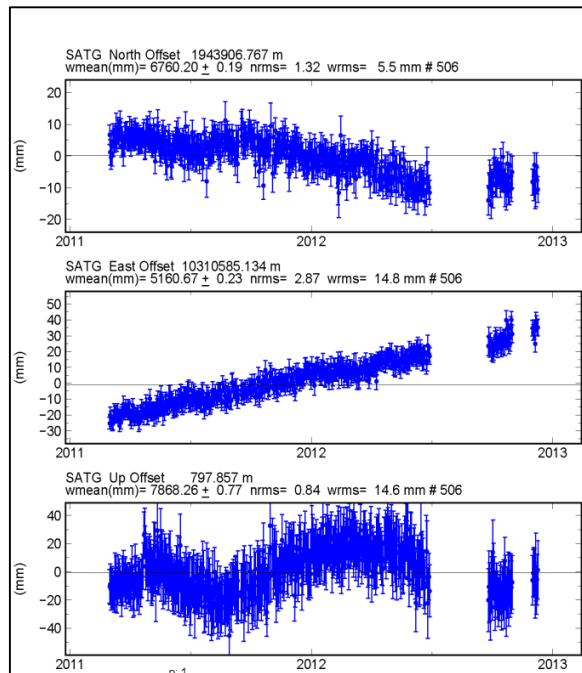


Figure 4.4 Time series of the Myanmar continuous GPS station (SATG)

The time series of the SATG is started in March 2011. Those four years of time series with a day sampling of the north, east and up coordinate components. The SATG station movement illustrates that is being pushed back toward the southeast (figure 4.4). The data gap involve in this time series graph due to a power supply problem.

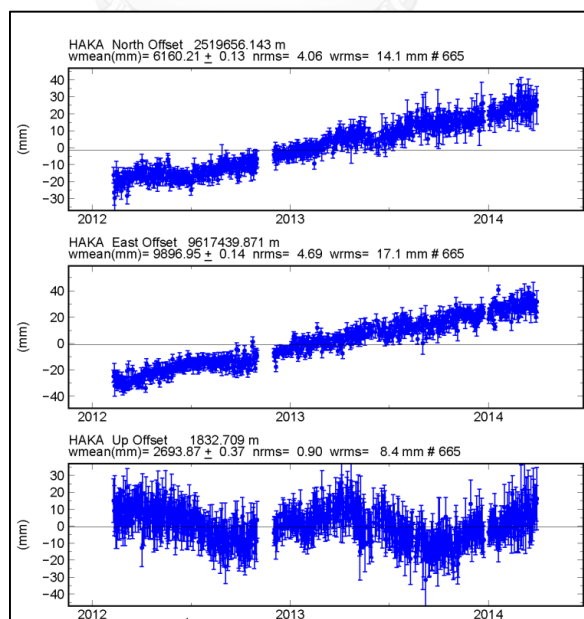


Figure 4.5 Time series of the Myanmar continuous GPS station (HAKA)

The HAKA station movements show that is being pushed back toward the northeast (figure 4.5).

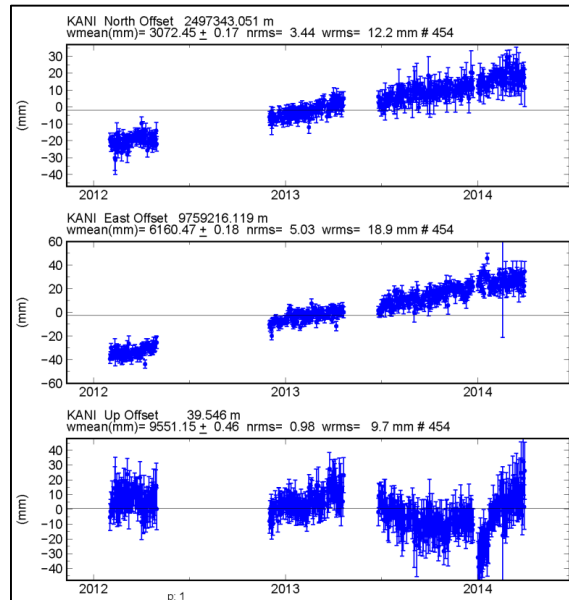


Figure 4.6 Time series of the Myanmar continuous GPS station (KANI)

Time series of the KANI plot with north, east and up coordinate components. Although the time series has a data gap and larger error bar, The KANI station movements prove that is being pushed back toward the northeast (figure 4.6).

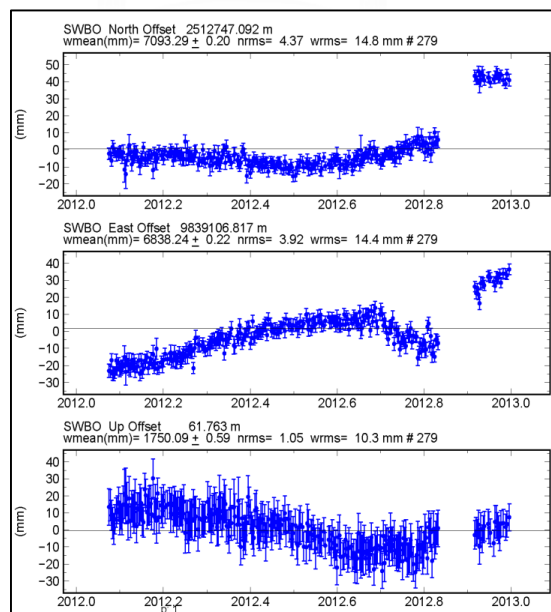


Figure 4.7 Time series of the Myanmar continuous GPS station (SWBO)

The SWBO time series graph movement immediately changes the position in November 2012. This displacement affected by the M 6.8 Thebeikkyin Earthquake. Graph GPS movement shows that is being pushed back toward the northeast by the west side of the Sagaing fault (figure 4.7).

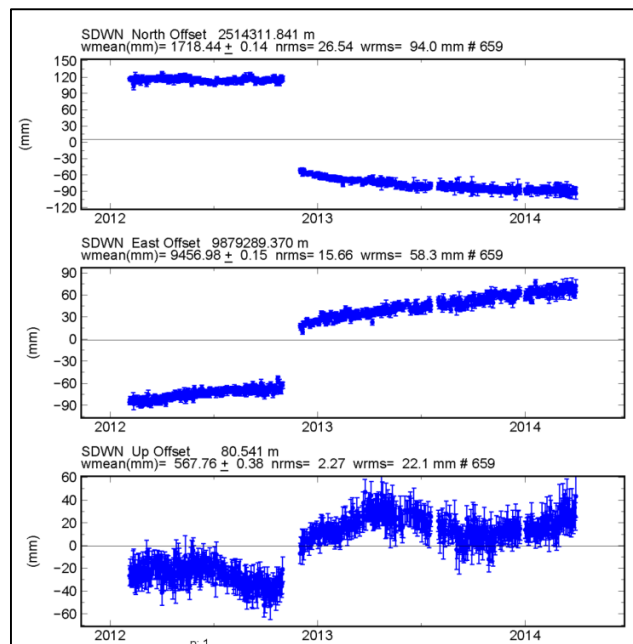


Figure 4.8 Time series of the Myanmar continuous GPS station (SDWN)

Time series of SDWN station also affected by the earthquake. Graph GPS movements prove that is being pushed back toward the southeast (figure 4.7). To get the post-seismic motion rates of the SWBO and SDWN stations, the study was used TRACK kinematic program for these two stations.

4.2. Comparing GPS results and discussion

The comparing step is adding one or more GPS stations results into one time series plot by using the append option from the GGMatlab. It is obvious to see the movement of better stations. In this research the combination of the east side station, which is northern transects the SATG and WAAW stations has similar moving rates. This two station direction is towards to the northeast (figure 4.9). There has been a bit difference between the movements of the eastern side of the Sagaing fault which are IGLE and GYBU stations, motion direction is same but GYBU station is moving more

than IGLE station (see in figure 4.10). Likewise HAKA, KANI and SWBO stations which are southern transect of the Sagaing fault (figure 4.11). They are located on the western side of the Sagaing fault, are differ due to the earthquake. The eastern side is the only one station in SDWN. So, it has nothing to compare.

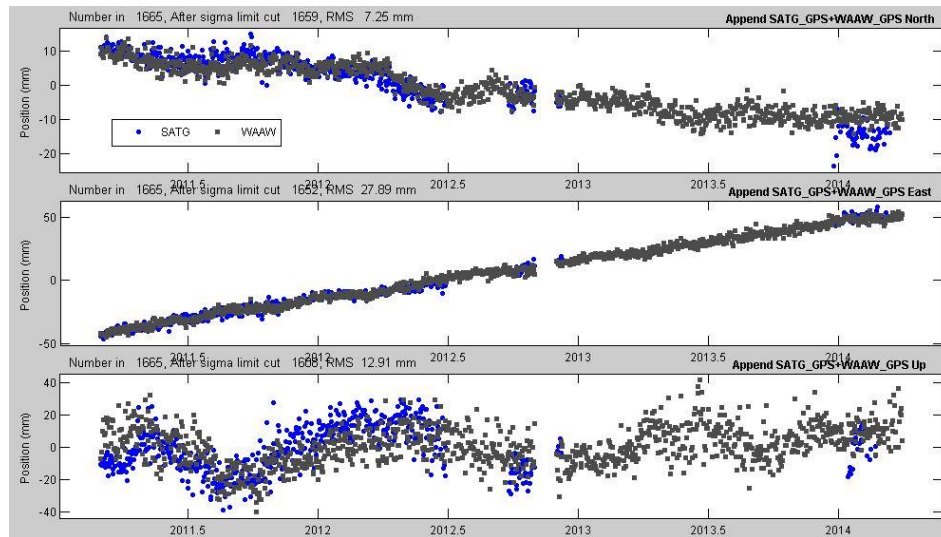


Figure 4.9 Comparing two stations time series (between the SATG and WAAW stations).

This time series compares the moving rate between SATG station (blue) and WAAW station (black) from 2011 to 2014. Overall, moving rate of these two stations is nearly the same rate.

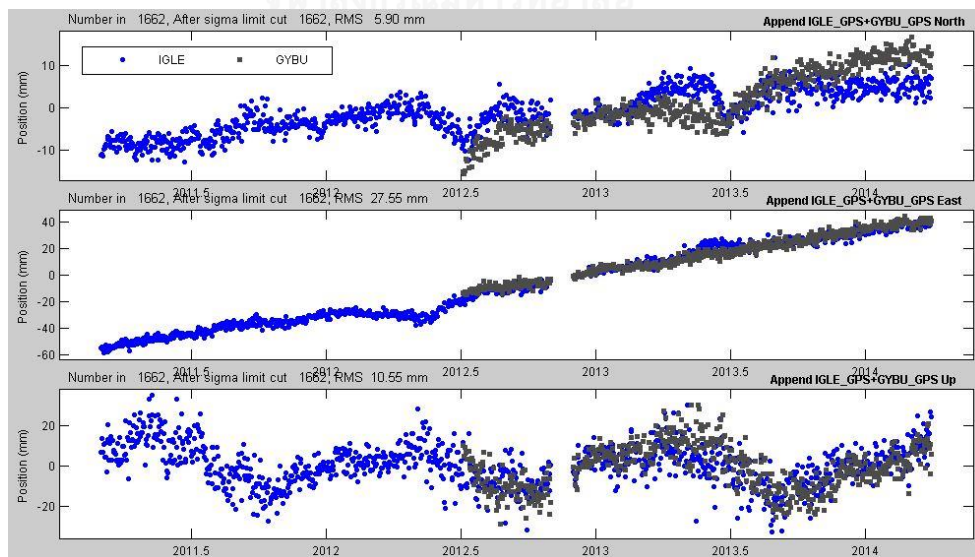


Figure 4.10 Comparing two stations time series (between the IGLE and GYBU stations).

This time series compares the moving rate between IGLE station (blue) and GYBU station (black) from 2011 to 2014. Overall, moving rates were small amount higher in the IGLE station than the GYBU stations.

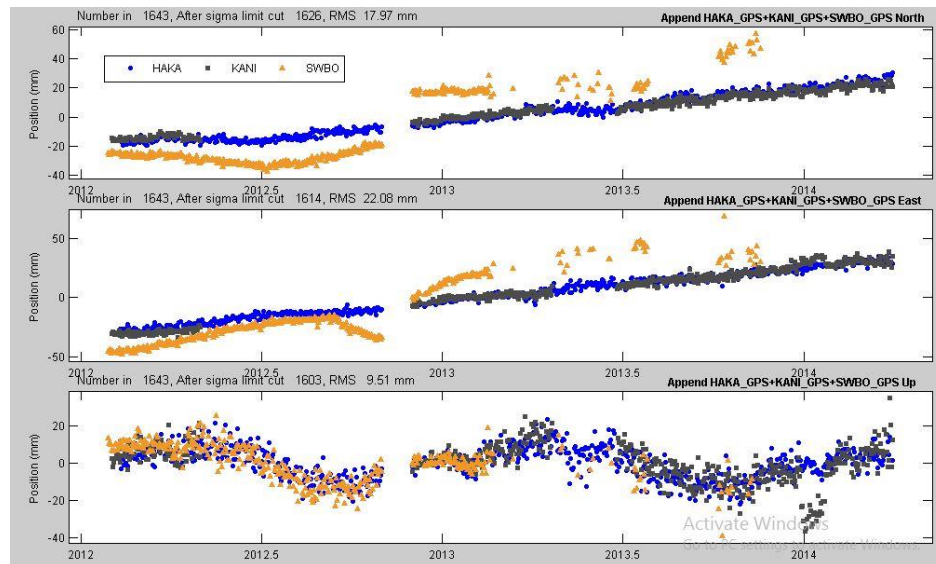


Figure 4.11 Comparing three stations time series (between the HAKA, KANI and SWBO stations).

This time series compares the moving rate between HAKA station (blue), KANI station (black) and GYBU station (yellow) from 2012 to 2014. Overall, it can be seen that the HAKA station and KANI station are nearly same in moving rate. The SWBO station is slower than the other two in moving rate, and 2012, November; the time series is immediately changed because of the Thabeikkyin earthquake.

4.3. Measuring Displacement due to the Thabeikkyin Earthquake

When an earthquake occurs, the fault moves instantaneously. The GPS measurements enable to determine the length of these displacements (Figure 4.5) and determine how much slip took place on the fault and where slip occurred. The GPS measurements show that the fault continues to slip slowly for months to years after an earthquake.

Post seismic motions are included in the above shown result of SWBO station and SDWN station (in section 4.1). Therefore, the moving rate will be in a large amount because the M 6.8 earthquake in 12, November 2012 occurred near the northern

transect. Initial results of the northern cGPS transect especially at the SWBO and SWDN stations (closest to the 2012 earthquake source). These two stations were immediately changed of position rate of 3 cm north and 15 cm south respectively.

In order to extract these post seismic motion, the motion occurred during the earthquake were calculated, using the break option for GGMatlab program. When using this method to calculate the annual motion rate, The SWBO station is moving at the north offset rate of 6.19 ± 2.77 mm/yr and east offset rate of 36.34 ± 1.47 mm/yr (Figure 4.1). The SDWN station is moving at the north offset rate of -21.11 ± 0.89 mm/yr and east offset rate of 34.69 ± 0.46 mm/yr.

4.4. Velocity Vector

Velocity can be represented an arrow, whose length equals the rate of motion and the direction of motion. These arrows are called a vector that describes rate and directions of motion. In this research first calculate for velocities for each local cGPS station in millimeter per year. Then the velocities in the form of vectors were placed on the map. For GPS velocity vector data may have two components (North and East) or three components including vertical, and in that study the Myanmar cGPS network map plotted velocity vectors in 2D. The velocity vector in two components (North and East) results would be shown in every station (shown in table 4.1).

Table 4-1 Moving rate of Myanmar cGPS network

Stations	North offset rate (mm/yr)	East offset rate (mm/yr)
GYBU	13.12 ± 0.20	31.74 ± 0.18
IGLE	4.51 ± 0.09	31.66 ± 0.14
WAAW	-6.92 ± 0.09	30.47 ± 0.08
SATG	-8.72 ± 0.15	31.23 ± 0.15
HAKA	21.50 ± 0.15	27.78 ± 0.13
KANI	17.89 ± 0.13	30.18 ± 0.17
SWBO	6.19 ± 2.77	36.34 ± 1.47
SDWN	-21.11 ± 0.89	34.69 ± 0.46

The velocity maps used to present the velocity and the direction of the GPS station. The present study calculated velocities for Myanmar cGPS stations in centimeters per year, using below graph (example for SWBO station). And then, all the results placed the velocities, in the form of vectors, on the Myanmar cGPS velocity map.

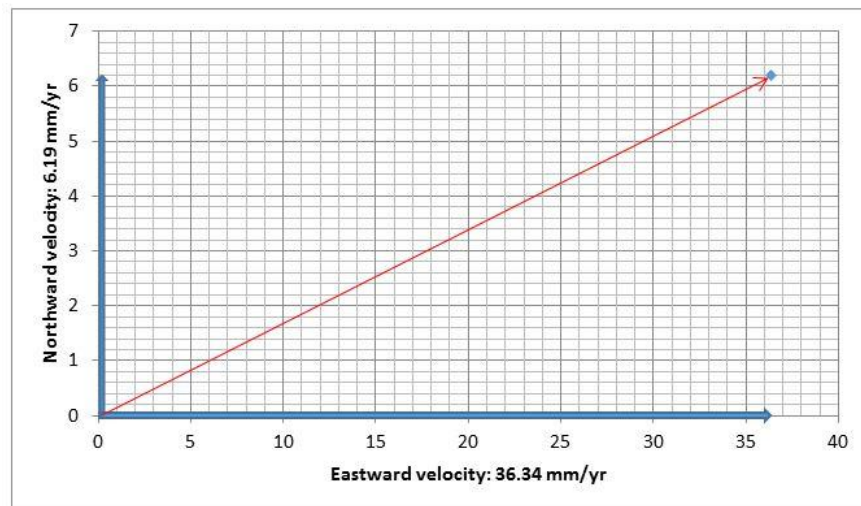


Figure 4.12 Example plot for the SWBO station

Plot the north (N) and east (E) vectors for the SWBO station on the grid and to determine that the movement was 36.86 mm/yr toward the northeast. Other GPS stations moving rate are shown in table 4.2.

Table 4-2 Based on time series results determine the moving rate of GPS stations.

Stations	Moving rate
GYBU	34.34 mm/yr toward the northeast
IGLE	31.98 mm/yr toward the northeast
WAAW	31.25 mm/yr toward the southeast
SATG	32.42 mm/yr toward the southeast
HAKA	35.13 mm/yr toward the northeast
KANI	35.08 mm/yr toward the northeast
SWBO	36.86 mm/yr toward the northeast
SDWN	40.61 mm/yr toward the southeast

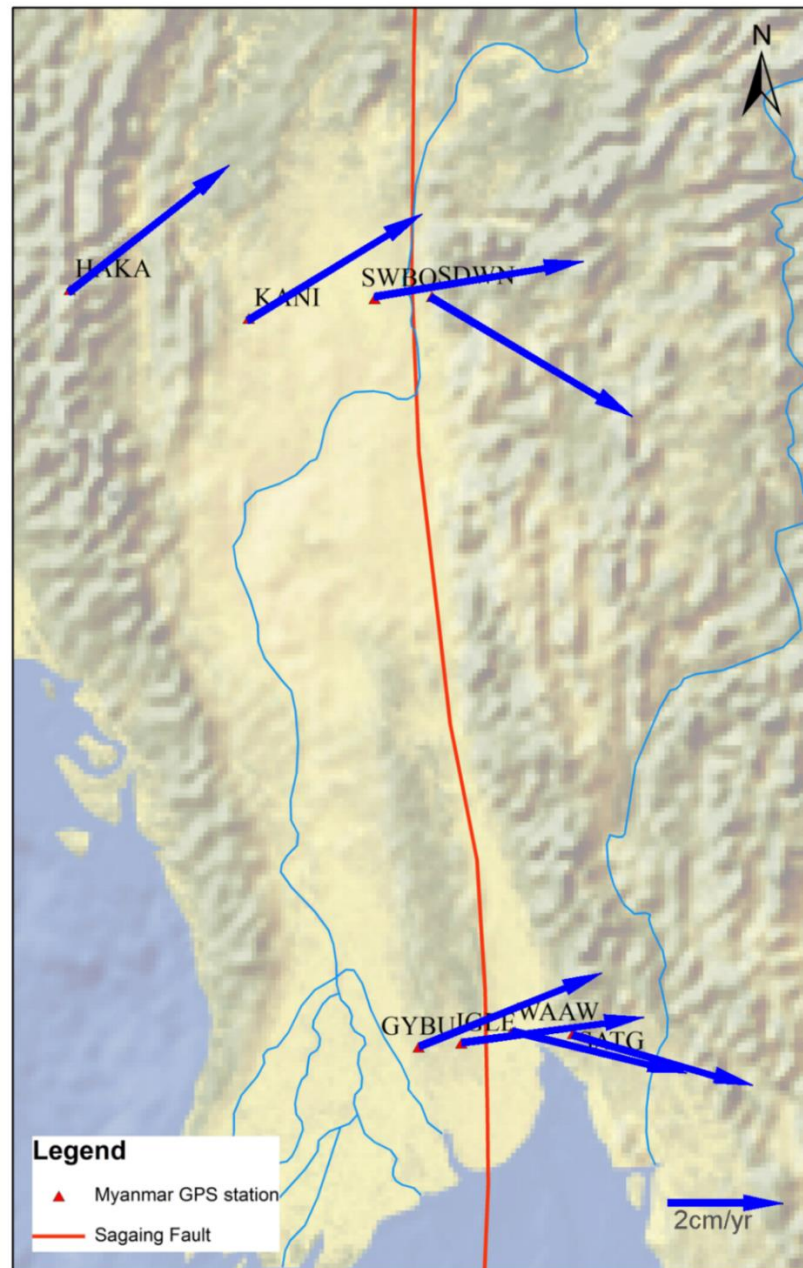


Figure 4.13 Velocity map for the Myanmar cGPS network

4.5. Kinematic Processing Results and discussion

The results of kinematic processing from the east-west component are illustrated in figure 4.15 and 4.16. These figures also show the ground motions derived from the GPS observations during the earthquake. High rate GPS data have been used to calculate the GPS data; therefore the motion rate is easily noticeable. The figure 4.15 shows the moving rates of the Thebeikkyin earthquake of magnitude 6.8 for the

SDWN station. And also the figure 4.9 illustrates the moving rate and direction of the SWBO station. After the comparison of the GAMIT/GLOBK processing and TRACK kinematic processing results, the results found that the SDWN station is moving to the south about 15 cm and the SWBO station is moving to the north about 3 cm.

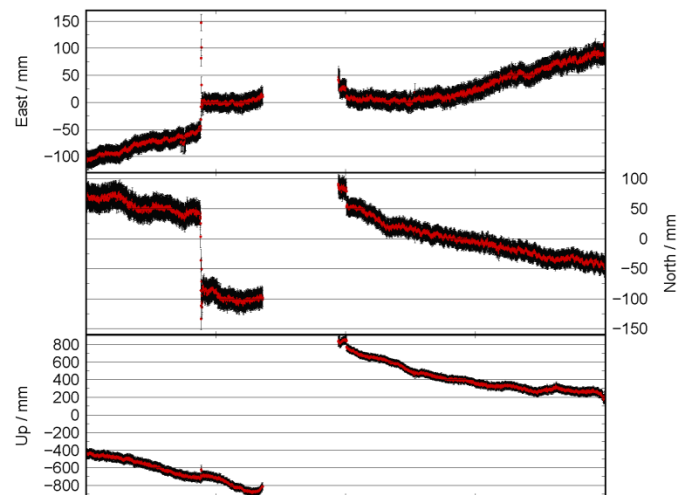


Figure 4.14 Kinematic processing result of SDWN station

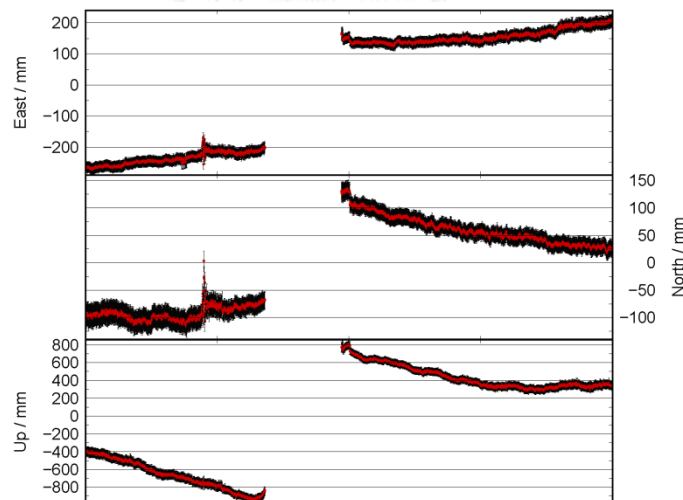


Figure 4.15 Kinematic processing result of SWBO station

Currently, the kinematic processing results obtained for post seismic movement rates of deformation regions have confirmed the results of GAMIT/ GLOBK processing. To give an opinion on every cGPS result shown above sections, roughly, the west side of the Sagaing fault is in moving to the north whereas the east side is moving to the east. The southern transect GPS stations, GYBU and IGLE which are from the west side of the Sagaing fault's moving rates are lower than the HAKA and KANI stations of the

northern transect. Likewise the moving rate of SATG and WAAW from eastern section is lower the SDWN station. One can see clearly on a velocity map.

The results from the GPS stations of the Myanmar cGPS network are not enough to clarify the slip rate of the Sagaing fault. Hence, Vigny measurement between 1998 and 2000 it is known that the measurement of central Myanmar near the Mandalay area, the Sagaing fault is at the moving rate of strike slip motion 18-20 mm/yr annually (Vigny, Socquet et al. 2003). According to the Vigny results, the displacements of the southern transect stations moving rates are still less than expected. This result requires further investigation to elucidate the cause for the observed deformation of the Sagaing fault.



CHAPTER 5

CONCLUSIONS AND RECOMMENDATION FOR FURTHER STUDY

5.1. Conclusion

The main point of this research was to process the Myanmar cGPS network by using with GAMIT, GLOBK and TRACK program. Analysis of Myanmar cGPS data collected at 8 stations in the northern and southern part of Myanmar across the Sagaing fault from 2011 to 2014. The movement of SWBO station and SDWN station from the northern transect were moving north during the 2012 November earthquake at least 3 cm and 15 cm respectively.

The present study processed the Myanmar cGPS data to get the moving rate of the GPS stations, According to the results; this GPS network can monitor the moving rate of the tectonic activity of the Sagaing fault, which is the fault critically important to study. Most of Myanmar's earthquakes originated from the Sagaing fault and furthermore there are tectonic activities yet to study. Myanmar's congested urban cities lie along the Sagaing fault, that's why it is the best way to observe the tectonics through GPS observations. As this Sagaing fault is around 1200 km in length, one needs more GPS stations to monitor the Sagaing fault. However, the results from using eight GPS stations are also supportive.

The GAMIT, GLOBK and TRACK program originated from MIT, which are very useful and powerful analysis software in GPS processing. With processing 24hr session RINEX data from Myanmar cGPS stations and RINEX files from 13 IGS stations have been combined and computed. The results obtained from quasi-observation files from GAMIT are known for the best square inversion in GAMIT and is suggested that the value of a posteriori variance factor (postfit rms) should not overtake 0.25 (King and Bock 1999). So in this research, our daily solutions were determined to overtake 0.25 of a posteriori variance factor values. Daily constrained solutions obtained by the GAMIT have been combined by using the GLOBK. The time series was taken out by using the generic mapping tool (GMT) of the GLOBK processing results, as well as by

using the GGMatlab program, time series are combined into a plot and moving rates were compared.

Later moving rate has been found by breaking the motion of the earthquake. The study observed four years of continuous GPS data between 2011 and 2014. It was found that the east side of the Sagaing fault the moving toward the southeast with the average rate of approximately 32-40 mm/yr and the other side of the fault the moving to the northeast with the rate of about 31-35 mm/yr. The details of results are already shown in chapter 4. In this way of study can investigate the earthquake offset clearly. Accordance with the aim of this research, using the GPS observation, the Sagaing fault's tectonic activities can be monitored. Furthermore, not only the GAMIT, GLOBK and TRACK program, but also step by step processing can be shown. By gaining continuous GPS, it is supportive in monitoring the Sagaing fault. In conclusion, suggest that this method is useful in many ways to make a research on monitoring the Sagaing fault tectonic actives in Myanmar.

5.2. Recommendation for Further Study

In that case of monitoring the Sagaing fault with the Myanmar cGPS network not sufficient to calculate a slip rate along the whole fault because the Sagaing fault is very long and there are not many GPS stations in Myanmar. The Sagaing fault is needed to investigate whether it is active is possible to do by using the GPS campaign. Furthermore, next processing for Myanmar GPS observation should be used both GMAIT/GLOBK and other powerful analysis software such as GIPSY and Bernese. And, the GIPSY is developed by the Jet Propulsion Laboratory (JPL). The Bernese GNSS Software is a scientific, high-precision, multi-GNSS data processing software developed at the Astronomical Institute of the University of Bern (AIUB). GNSS stands for Global Navigation Satellite System, that term includes example the GPS, GLONASS, Galileo, Beidou and other regional systems. Next analysis for the Sagaing fault should use not only the GPS but also GNSS system for more reliable results.

REFERENCES

Altamimi, Z., et al. (2011). "ITRF2008: an improved solution of the international terrestrial reference frame." Journal of Geodesy **85**(8): 457–473.

Altamimi, Z., et al. (2002). "ITRF2000: A new release of the International Terrestrial Reference Frame for earth Science applications." journal of Geophysical Research **107**(B10): 2214.

Aung, H. H. (2015). Myanmar Earthquake History Myanmar.

Bender, P. L. and D. R. Larden (1985). GPS carrier phase ambiguity resolution over long baselines. Proceedings of the First International Symposium on Precise Positioning with the Global Positioning System. G. C. C. **1**: 357-361.

Bertrand, G., et al. (1998). "The Singu basalts (Myanmar): new constraints for the amount of recent offset on the Sagaing Fault." Earth and Planetary Science **327**: 479–484.

Beutler, G., et al. (2007). Bernese GPS Software, Version 5.0. Astronomical Institute, University of Bern.

Bird, P. (2003). "An updated digital model of plate boundaries." Geochemistry, GeoPhysics, Geosystems **4**(1027): doi:10.1029/2001GC000252.

Blewitt, G. (1990). "An automatic editing algorithm for GPS data." Geophysical Research Letters.

Blewitt, G. (1997). Basics of the GPS Technique: Observation Equations. Nordic Geodetic Commission, Sweden.

Bock Y., S. A. G., C. C. Counselman III, R. W. King, R. I. Abbot (1986). "Interferometric analysis of GPS phase observation." Manuscripta Geodaetica **11**: 282-288.

Curry, J. R. (2005). "Tectonics and history of the Andaman Sea region." Journal of Asian Earth Sciences **25**(1): 187–232.

Curry, J. R., et al. (1982). Structure, tectonics, and geological history of the northeastern Indian Ocean.

Curry, J. R., et al. (1979). "Tectonics of the Andaman Sea and Burma." **29**: 189–198.

Dain, A. Y. L., et al. (1984). "Active faulting and tectonics of Burma and surrounding regions." Journal of Geophysical Research **89**(B1): 453–472.

Dana, P. H. (2000). "Global Positioning System Overview." from http://www.colorado.edu/geography/gcraft/notes/gps/gps_f.html.

Dong, D.-N., Y. Bock (1989). "GPS network analysis with phase ambiguity resolution applied to crustal deformation studies in California." J. geophys. Res., **94**: 3949-3966.

Estey, L. H. and C. M. Meertens (1999). "TEQC: The Multi-Purpose Toolkit for GPS/GLONASS Data." GPS Solutions (pub. by John Wiley & Sons) **3**(1): 42-49.

Herring, T. (1999). Documentation for the GLOBK software version 5.01. Mass. Inst. of Technol., Cambridge, .

Herring, T. (2003). "MATLAB tools for viewing GPS velocities and time series." GPS Solutions (pub. by John Wiley & Sons) **7**: 194-199.

Herring, T., et al. (2010). Introduction to GAMIT/GLOBK.

Khan, P. K. and P. P. Chakraborty (2005). "Two-phase opening of Andaman Sea: a new seismotectonic insight." Earth and Planetary Science Letters **229**(3-4): 259-271.

King, R. W. and Y. Bock (1999). Documentation for the GAMIT GPS software analysis version 9.9. Mass. Inst. of Technol., Cambridge.

Langley, R. B. (1997). "The GPS error budget." GPS World **8**(3): 51-56.

Liu, Z. and P. Bird (2008). "Kinematic modeling of neotectonics in the Persia-Tibet-Burma orogen." Geophys. J. Int. **172**(2): 779-797.

McClusky, S., et al. (2000). "Global Positioning System constraints on plate motions and deformations in eastern Mediterranean and Caucasus." journal of Geophysical Research **105**(B3): 5695-5719.

McClusky, S., et al. (2003). "GPS constraints on Africa (Nubia) and Arabia plate motions." Geophysical Journal International **155**: 126-138.

Meade, B. J. (2007). "Present-day kinematics at the India-Asia collision zone." Geology **35**(1): 81–84.

Mitchell, A. H. G., et al. (2007). "Rock relationships in the Mogok metamorphic belt, Tatkon to Mandalay, central Myanmar." Journal of Asian Earth Sciences **29**(5-6): 891-910.

Morley, C. K. (2004). "Nested strike-slip duplexes, and other evidence for Late Cretaceous–Palaeogene transpressional tectonics before and during India–Eurasia collision, in Thailand, Myanmar and Malaysia." Journal of the Geological Society **161**(5): 799-812.

Reilinger, R., et al. (2006). "GPS constraints on continental deformation in the Africa-Arabia-Eurasia continental collision zone and implications for the dynamics of plate interactions." Journal of Geophysical Research **111**(B05).

Ridd, M. F. and I. Watkinson (2013). "The Phuket-Slate Belt terrane: tectonic evolution and strike-slip emplacement of a major terrane on the Sundaland margin of Thailand and Myanmar." Proceedings of the Geologists' Association **124**(6): 994-1010.

Searle, M. P. and C. K. Morley (2011). "Tectonic and thermal evolution of Thailand in the regional context of SE Asia." (Geology of Thailand. Geological Society of London Memoir): 539-572.

Socquet, A., et al. (2006). "India and Sunda plates motion and deformation along their boundary in Myanmar determined by GPS." journal of Geophysical Research **111**(B5).

Thein, M., et al. (1991). On the lateral displacement of the Sagaing fault. Georeport. **1(1)**: 23–34.

Tun, S. T. and M. Thein (2012). Tectonic Map of Myanmar 2012. Presentation at GeoMyanmar, Yangon, Myanmar, March 2012.

Vaniček, P. and E. J. Krakiwsky (1986). Geodesy: The Concepts. New York: North-Holland.

Vigny, C., et al. (2002). "GPS network monitors the Western Alps deformation over a five-year period: 1993-1998." Journal of Geodesy **76**(2): 63-76.

Vigny, C., et al. (2003). "Present-day crustal deformation around Sagaing fault, Myanmar." journal of Geophysical Research **108**(B11): 2533.

Wang, Y., et al. (2013). "Permanent upper plate deformation in western Myanmar during the great 1762 earthquake: Implications for neotectonic behavior of the northern Sunda megathrust." journal of Geophysical Research **118**(3): 1277-1303.

Wang, Y., et al. (2011). "Earthquakes and slip rate of the southern Sagaing fault: insights from an offset ancient fort wall, lower Burm (Myanmar)." Geophysical Journal International **185**(1): 49-64.

Watkinson, I., et al. (2011). "The timing of strike–slip shear along the Ranong and Khlong Marui faults, Thailand." journal of Geophysical Research **116**(B9).

Yeats, R. S., et al. (1997). *The Geology of Earthquakes*. New York, NY, Oxford Press.





APPENDIX

จุฬาลงกรณ์มหาวิทยาลัย
CHULALONGKORN UNIVERSITY

Appendix A: List of GAMIT processing files (Herring, King et al. 2010)

- A - file: ASCII version of the T-file (tabular ephemeris)
- B - file: controls the batch mode of data processing
- C - file: observed – computed (O-C's), partial derivatives
- D - file: driver file of sessions and receivers
- E - file: broadcast ephemeris, in FICA Blk 9 or RINEX navigation file format
- G - file: orbital initial conditions and non-gravitational parameter values
- H - file: adjustments and full variance-covariance matrix for input to GLOBK
- I - file: receiver clock polynomial input
- J - file: satellite clock polynomial coefficients
- K - file: values of receiver clock offset during observation span, from pseudorange
- L - file: station coordinates
- M - file: controls merging of data (C-) files for SOLVE and editing programs
- N - file: data-weight overrides for SOLVE created from autcln.sum.postfit
- O - file: record of the analysis (reduced form of Q-file) for post-processing analysis
- P - file: record of a MODEL run
- Q - file: record of the analysis (SOLVE run)
- S - file: station coordinates and antenna offsets — no longer used
- T - file: tabular ephemeris
- V - file: editing output of SINCLN, DBLCLN, and SCANRMS
- W - file: meteorological data
- X - file: input observations
- Y - file: satellite yaw parameters
- Z - file: water-vapor radiometer data

Appendix B: session info

<p>Session Table</p> <p>Processing Agency = MIT</p> <p>Satellite Constraint = Y ; Y/N (next two lines are free-format but 'all' must be present)</p> <pre style="margin-left: 40px;"> all a e i n w M rad1 rad2 rad3 rad4 rad5 rad6 rad7 rad8 rad9; 0.01 0.01 0.01 0.01 0.01 0.01 0.01 0.01 0.01 0.01 0.01 0.01 0.01 0.01 </pre> <p><< Controls must begin in column 1 >></p> <p>Choice of Experiment = BASELINE ; BASELINE/RELAX./ORBIT</p> <p>Type of Analysis = 1-ITER ; 1-ITER(autcln prefit and conditional redo) / 0-ITER (no postfit autcln) / PREFIT</p> <p>AUTCLN redo = Y ; Y/N; 3rd soln only if needed, assume 'Y' if 'Type of analysis = 1-ITER'</p> <p>Choice of Observable = LC_AUTCLN ; LC_AUTCLN (default), LC_HELP (codeless L2), L1_ONLY (L1 soln from dual freq),</p> <pre style="margin-left: 40px;"> L2_ONLY (L2 soln from dual freq), L1,L2_INDEPENDENT (L1 + L2 from dual freq) L1&L2 (same as L1,L2_INDEPENDENT but with ion constraint); L1_RECEIVER (must add 'L1only' in autcln.cmd) </pre> <p>Station Error = ELEVATION 10 5 ; 1-way L1, $a^{**2} + (b^{**2})/(\sin(\text{elev})^{**2})$ in mm. default = 10. 0.</p> <p>AUTCLN reweight = Y ; Y/N; reweight data from autcln rms; replaces 'Use N-file' in releases < 10.32</p> <p>AUTCLN Command File = autcln.cmd ; Filename; default none (use default options)</p> <p>Decimation Factor = 4 ; FOR SOLVE, default = 1</p> <p>Quick-pre decimation factor = 10 ; 1st iter or autcln pre, default same as Decimation Factor</p> <p>Quick-pre observable = LC_ONLY ; for 1st soln, default same as Choice of observable</p> <p>Ionospheric Constraints = 0.0 mm + 8.00 ppm</p> <p>Ambiguity resolution WL = 0.15 0.15 1000. 99. 15000. ; for LC_HELP, ignored for LC_AUTCLN</p> <p>Ambiguity resolution NL = 0.15 0.15 1000. 99. 15000. ; allow long baselines with LC_AUTCLN</p> <p>Zenith Delay Estimation = Y ; Yes/No (default No)</p> <p>Interval zen = 2 ; 2 hrs = 13 knots/day (default is 1 ZD per day)</p> <p>Zenith Constraints = 0.50 ; zenith-delay a priori constraint in meters (default 0.5)</p> <p>Zenith Variation = 0.02 100. ; zenith-delay variation, tau in meters/sqrt(hr), hrs (default .02 100.)</p> <p>Elevation Cutoff = 10 ; default 0 to use value in autcln.cmd</p>

Atmospheric gradients = Y ; Yes/Np (default No)
 Number gradients = 2 ; number of gradient parameters per day (NS or ES); default 1
 Gradient Constraints = 0.01 ; gradient at 10 deg elevation in meters; default 0.03 m

 Update T/L files = L_ONLY ; T_AND_L (default), T_ONLY, L_ONLY, NONE
 Update tolerance = .3 ; minimum adjustment for updating L-file coordinates, default .3 m

 Met obs source = GPT 50 ; hierarchical list with humidity value at the end; e.g. RNX UFL GPT 50 ; default
 GTP 50

 if [humid value] < 0, use RNX or UFL if available
 Output met = N ; write the a priori met values to a z-file (Y/N)
 Use met.list = N ; not yet supported
 Use met.grid = N ; not yet supported
 DMap = GMF ; GMF(default)/NMFH/VMF1
 WMap = GMF ; GMF(default)/NMFV/VMF1
 Use map.list = N ; VMF1 list file with mapping functions, ZHD, ZWD, P, Pw, T, Ht
 Use map.grid = N ; VMF1 grid file with mapping functions and ZHD
 Yaw Model = Y ; Y/N default = Y
 Radiation Model for ARC = BERNE
 Inertial frame = J2000
 Tides applied = 31 ; Binary coded: 1 earth 2 freq-dep 4 pole 8 ocean 16 remove mean for pole
 tide
 ; 32 atmosphere ; default = 31
 Use otl.list = N ; Ocean tidal loading list file from OSO
 Use otl.grid = Y ; Ocean tidal loading grid file, GAMIT-format converted from OSO
 Etide model = IERS03 ; IERS96/IERS03
 Earth Rotation = 11 ; Diurnal/Semidirunal terms: Binary coded: 1=pole 2=UT1 4=Ray model;
 8=IERS2010 ; default=11
 Apply atm loading = N ; Y/N for atmospheric loading
 Use atmL.list = N ; Atmospheric (non-tidal) loading list file from LU
 Use atmL.grid = N ; Atmospheric (non-tidal) loading grid file from LU, converted to GAMIT format
 Use atL.list = N ; Atmospheric tides, list file, not yet available
 Use atL.grid = N ; Atmospheric tides, grid file

 Antenna Model = AZEL ; NONE/ELEV/AZEL default = ELEV Use AZEL for IGS absolute ANTEX files
 SV antenna model = ELEV ; NONE/ELEV default = NONE Use ELEV for IGS ANTEX files

SV antenna off = N ; Y/N to estimate satellite antenna offsets (default N)

Delete AUTCLN input C-files = Y ; Y/N ; default Y to force rerun of MODEL

Scratch directory = /tmp

<< List of additional controls not commonly - blank first column to indicate a comment >>

Simulation con : s-file name

Inertial frame = B1950 ; B1950/J2000 (default = J2000)

Initial ARC ; Y/N default = Yes

Final ARC ; Y/N default = No

Radiation Model for ARC ; SPHRC/BERNE/SRDYB/SVBDY default = SPHRC

Reference System for ARC ; WGS72/WGS84/MERIT/IGS92/EGM96/EGM08(incremental_updates) (default = EGM08)

Tabular interval for ARC ; 900. seconds (new default), 1350. seconds (old default)

Stepsize for ARC ; 75. seconds (new default), 168.75 seconds (old default)

Arc debug flag : Turn on various print and test options (see arc.f) (default = 0)

Earth Rotation ; Diurnal/Semidirunal terms: Binary coded: 1=pole 2=UT1 4=Ray model; 8=IERS2010 ; default=11

Estimate EOP ; Binary coded: 1 wob 2 ut1 4 wob rate 8 ut1 rate

Wobble Constraint = 3. 0.3 ; Default 3. (arcsec) 0.3 (arcsec/day)

UT1 Constraint = 0.00002 0.02 ; Default .00002 (sec) 0.02 (sec/day)

Number Zen = 4 ; number of zenith-delay parameters (default 1)

Zenith Constraints = 0.50 ; zenith-delay a priori constraint in meters (default 0.5)

Zenith Model = PWL ; PWL (piecewise linear)/CON (step)

Zenith Variation = 0.02 100. ; zenith-delay variation, tau in meters/sqrt(hr), hrs (default .02 100.)

Gradient Constraints = 0.03 ; gradient at 10 deg elevation in meters

Gradient Variation = .01 100 ; gradient variation

Tropospheric Constraints = NO ; YES/NO (spatial constraint)

Ion model = NONE ; NONE/GMAP (default NONE) use 2nd/3rd order ionospheric corrections

Mag field = IGRF11 ; ITRF11/IGRF10/DIPOLE (default IGRF11)

Yaw Model	; YES/NO default = YES
I-file = N	; Use I-file (Y/N) (default Y)
AUTCLN Postfit = Y	; Assume 'Y' if 'Type of analysis = 1-ITER' (autcln.cmd.postfit file also)
Delete AUTCLN input C-files = Y	; YES/NO/Intermediate (default no)
AUTCLN Command File	; Filename; default none (use default options)
Delete eclipse data = POST	; ALL/NO/POST (Default = NO)
SCANDD control	; BOTH (default) /NONE/FIRST/FULL/IFBAD see manual sec. 5.2
Iteration	; CFILES / XFILES (default)
Edit AUTCLN Command File	; YES/NO; default = NO (For clocks, no longer needed)
Ambiguity resolution WL	; default = 0.15 0.15 1000. 10. 500.
Ambiguity resolution NL	; default = 0.15 0.15 1000. 10. 500.
Type of Biases	: IMPLICIT (default for quick), EXPLICIT (default for full)
H-file solutions	; ALL ; LOOSE-ONLY
Skip loose	: Y / N (default) sometimes necessary for short baselines
Station Error = BASELINE 10. 0.	; 1-way L1, $a^{**2} + (b^{**2})(L^{**2})$ in mm, ppm, default = 10. 0.
Station Error = UNIFORM 10.	; 1-way L1 in mm, default = 10.
Station Error = ELEVATION 4.3 7.0	; 1-way L1 , $a^{**2} + b^{**2}/\sin(\text{elev})^{**2}$ in mm, default = 4.3 7.0
Satellite Error = UNIFORM 0.	; 1-way L1 in mm (added quadratically to station error) default = 0.
Select Epochs	; Enter start and stop epoch number (applies only to SOLVE)
Decimation Factor	; FOR SOLVE, default = 1
Elevation Cutoff = 15.	; For SOLVE, overrides the MODEL or AUTCLN values if they are lower
Correlation print	; Threshold for printing correlations (default 0.9999)
Export Orbits	; YES/NO default = NO
Orbit id	; 4-char code read only if Export Orbits = YES
Orbit Format	; SP1/SP3 (NGS Standard Products)
Orbit organization	; 3-char code read only if Export Orbits = YES
Reference System for Orbit = ITR93	; ITR92/ITR91/ITR90/WGS84/MERIT (for SP3 header)
Lunar eclipses = Y	; Set = N to turn off lunar eclipses in ARC to match model of GAMIT < 10.2 (default Y)
	(no longer supported: see arc_debug below)
Delete all input C-files	; YES/NO default = NO
Delete MODEL input C-files	; YES/NO default = NO
Delete AUTCLN input C-files	; YES/NO default = NO

Update T/L files	; T_AND_L (default), T_ONLY, L_ONLY, NONE (Applies only to update for final solution after initial)
Update tolerance	; minimum adjustment for updating L-file coordinates, default .3 m
SOLVE-only = YES	; YES/NO default = NO
X-compress = YES	; Uncompress/compress X-files default = NO
SCANDD control	; FULL (default), FIRST, BOTH, IFBAD, NONE
Run CTOX = YES	; Make clean X-files from C-files default = NO
Bias apriori = 100.	; Optional constraint on biases for LC_AUTCLN (default 0 -> no constraint)
SOLVE print = Y	; Turn on SOLVE output to screen (default N)
Bias apriori = 1000.	; Optional constraint on biases for LC_AUTCLN (default 1000, 0 -> constraint)
Bias rcond = 10000.	; Condition number ratio for fixing dependent biases (default 10000.)



Appendix C: station.info

```
# stationextract.php written by user albertyw    on 2013-12-23 10:21

* Reference file: database

* IGS Log File : cshr.log

*

*

*SITE Station Name      Session Start   Session Stop   Ant Ht   HtCod  Ant N   Ant E   Receiver Type
Vers          SwVer Receiver SN      Antenna Type   Dome  Antenna SN
0001 GEONET0001      2011 60 0 0 0 9999 999 0 0 0 0.0000 DHARP  0.0000 0.0000 TRIMBLE NETR9
Nav 4.17 Sig 0.00   4.17 ----- TRM29659.00  GSI -----
0002 GEONET0002      2011 60 0 0 0 9999 999 0 0 0 0.0000 DHARP  0.0000 0.0000 TRIMBLE NETR9
Nav 4.17 Sig 0.00   4.17 ----- TRM29659.00  GSI -----
0003 GEONET0003      2011 60 0 0 0 9999 999 0 0 0 0.0000 DHARP  0.0000 0.0000 TRIMBLE 5700
Nav 1.24 Sig 0.00   1.24 ----- TRM29659.00  GSI -----
0004 GEONET0004      2011 60 0 0 0 9999 999 0 0 0 0.0000 DHARP  0.0000 0.0000 TRIMBLE 5700
Nav 1.24 Sig 0.00   1.24 ----- TRM29659.00  GSI -----
0005 GEONET0005      2011 60 0 0 0 9999 999 0 0 0 0.0000 DHARP  0.0000 0.0000 TRIMBLE 5700
Nav 1.24 Sig 0.00   1.24 ----- TRM29659.00  GSI -----
0007 GEONET0007      2011 60 0 0 0 9999 999 0 0 0 0.0000 DHARP  0.0000 0.0000 TRIMBLE 5700
Nav 1.24 Sig 0.00   1.24 ----- TRM29659.00  GSI -----
0008 GEONET0008      2011 60 0 0 0 9999 999 0 0 0 0.0000 DHARP  0.0000 0.0000 TRIMBLE 5700
Nav 1.24 Sig 0.00   1.24 ----- TRM29659.00  GSI -----
0009 GEONET0009      2011 60 0 0 0 9999 999 0 0 0 0.0000 DHARP  0.0000 0.0000 TRIMBLE 5700
Nav 1.24 Sig 0.00   1.24 ----- TRM29659.00  GSI -----
0010 GEONET0010      2011 60 0 0 0 9999 999 0 0 0 0.0000 DHARP  0.0000 0.0000 TRIMBLE NETR9
Nav 4.17 Sig 0.00   4.17 ----- TRM29659.00  GSI -----
0011 GEONET0011      2011 60 0 0 0 9999 999 0 0 0 0.0000 DHARP  0.0000 0.0000 TPS NETG3
3.4 EG3 Jul,02,2010 3.40 ----- TRM29659.00  GSI -----
0012 GEONET0012      2011 60 0 0 0 9999 999 0 0 0 0.0000 DHARP  0.0000 0.0000 TRIMBLE NETR9
Nav 4.17 Sig 0.00   4.17

ZWEN Astronomical Obs 1996 64 0 0 0 1999 251 16 0 0 0.0460 DHPAB 0.0000 0.0000 ROGUE SNR-
8000 3.2 3.20 270 AOAD/M_T NONE 342
ZWEN Astronomical Obs 1999 251 16 0 0 2000 251 0 0 0 0.0460 DHPAB 0.0000 0.0000 AOA SNR-
8000 ACT 3.3.32.3 3.30 245 AOAD/M_T NONE 342
ZWEN Astronomical Obs 2000 251 0 0 0 2000 265 0 0 0 0.0460 DHPAB 0.0000 0.0000 AOA SNR-
8000 ACT 3.3.32.3 3.30 279 AOAD/M_T NONE 342
ZWEN Astronomical Obs 2000 265 0 0 0 2016 365 0 0 0 0.0460 DHPAB 0.0000 0.0000 AOA SNR-
8000 ACT 3.3.32.3 3.30 279 AOAD/M_T NONE 237
```

IGLE	ingle station	2011 038 00 00 00	2016 365 00 00 00	0.0000	DHPAB	0.0000	0.0000	TRIMBLE	NETR8
4.15		--- 5025K68503	TRM29659.00	SCIS					
SATG	shanatetg station	2011 042 00 00 00	2016 365 00 00 00	0.0000	DHPAB	0.0000	0.0000	TRIMBLE	NETR8
4.15		--- 5021K67580	TRM29659.00	SCIS					
WAAW	waw station	2011 045 00 00 00	2016 365 00 00 00	0.0000	DHPAB	0.0000	0.0000	TRIMBLE	NETR8
4.15		--- 5025K68570	TRM29659.00	SCIS					
GYBU	gyophu station	2011 045 00 00 00	2016 365 00 00 00	0.0000	DHPAB	0.0000	0.0000	TRIMBLE	NETR8
4.15		--- 5202K81318	TRM29659.00	SCIS					
HAKA	hakha station	2012 020 00 00 00	2016 365 00 00 00	0.0000	DHPAB	0.0000	0.0000	TRIMBLE	NETR9
4.15		--- 5025K68571	TRM29659.00	SCIS					
KANI	kanni station	2012 020 00 00 00	2016 365 00 00 00	0.0000	DHPAB	0.0000	0.0000	TRIMBLE	NETR9
4.15		--- 5213K83713	TRM29659.00	SCIS					
SWBO	shewbo station	2012 020 00 00 00	2016 365 00 00 00	0.0000	DHPAB	0.0000	0.0000	TRIMBLE	NETR9
4.15		--- 5137K78283	TRM29659.00	SCIS					
SDWN	seldwin station	2012 020 00 00 00	2016 365 00 00 00	0.0000	DHPAB	0.0000	0.0000	TRIMBLE	NETR9
4.15		--- 5137K78324	TRM29659.00	SCIS					

Appendix D: Q - file: record of GAMIT analysis

Program SOLVE Version 10.48 2014/5/15 09:00 (Linux)

SOLVE Run on 2014/ 9/ 6 8:55:14

OWNER: MIT OPERATOR: pyae

Solution refers to : 2014/ 1/ 1 12: 0 (2014.0014)

Epoch interval: 1 - 2880

Decimation interval: 4

LC solution with AUTCLN bias-fixing

-Bias constraints = 1000. cycles

Cutoff elevation angle in SOLVE batch file (degrees):

Station	Cutoff angle
1 BAKO BAKOSURTANAL	0.00
2 COCO Cocos	0.00
3 CUSV Chulalongkor	0.00
4 DARW Darwin AU014	0.00
5 DGAR Diego Garcia	0.00
6 GYBU gyophu stati	0.00
7 HAKA hakha statio	0.00
8 IGLE ingle statio	0.00
9 IISC Indian Insti	0.00
10 KANI kanni statio	0.00
11 LCK2 Lucknow(Utta	0.00
12 LHAZ Lhasa	0.00
13 NTUS Nanyang Tech	0.00
14 PERT Perth	0.00
15 PIMO Manila Obser	0.00
16 SATG shanatetg st	0.00
17 SDWN seldwin stat	0.00
18 SWBO shewbo stati	0.00
19 WAAW waw station	0.00

A priori coordinate errors in meters

Station	Latitude	Longitude	Radius
1 BAKO BAKOSURTANAL	100.0000	100.0000	100.0000
2 COCO Cocos	0.0500	0.0500	0.0500
3 CUSV Chulalongkor	100.0000	100.0000	100.0000
4 DARW Darwin AU014	0.0500	0.0500	0.0500

5	DGAR Diego Garcia	0.0500	0.0500	0.0500	
6	GYBU gyophu stati	100.0000	100.0000	100.0000	
7	HAKA hakha statio	100.0000	100.0000	100.0000	
8	IGLE ingle statio	100.0000	100.0000	100.0000	
9	IISC Indian Insti	0.0500	0.0500	0.0500	
10	KANI kanni statio	100.0000	100.0000	100.0000	
11	LCK2 Lucknow(Utta	100.0000	100.0000	100.0000	
12	LHAZ Lhasa	0.0500	0.0500	0.0500	
13	NTUS Nanyang Tech	100.0000	100.0000	100.0000	
14	PERT Perth	0.0500	0.0500	0.0500	
15	PIMO Manila Obser	0.0500	0.0500	0.0500	
16	SATG shanatetg st	100.0000	100.0000	100.0000	
17	SDWN seldwin stat	100.0000	100.0000	100.0000	
18	SWBO shewbo stati	100.0000	100.0000	100.0000	
19	WAAW waw station	100.0000	100.0000	100.0000	
A priori zenith delay Model = PWL					
Station	#	A priori (m)	Markov (m/sqrt(hr))	Correlation time (hrs)	
1	BAKO BAKOSURTANAL	13	0.500	0.020	100.000
2	COCO Cocos	13	0.500	0.020	100.000
3	CUSV Chulalongkor	13	0.500	0.020	100.000
4	DARW Darwin AU014	13	0.500	0.020	100.000
5	DGAR Diego Garcia	13	0.500	0.020	100.000
6	GYBU gyophu stati	13	0.500	0.020	100.000
7	HAKA hakha statio	13	0.500	0.020	100.000
8	IGLE ingle statio	13	0.500	0.020	100.000
9	IISC Indian Insti	13	0.500	0.020	100.000
10	KANI kanni statio	13	0.500	0.020	100.000
11	LCK2 Lucknow(Utta	13	0.500	0.020	100.000
12	LHAZ Lhasa	13	0.500	0.020	100.000
13	NTUS Nanyang Tech	13	0.500	0.020	100.000
14	PERT Perth	13	0.500	0.020	100.000
15	PIMO Manila Obser	13	0.500	0.020	100.000
16	SATG shanatetg st	13	0.500	0.020	100.000
17	SDWN seldwin stat	13	0.500	0.020	100.000
18	SWBO shewbo stati	13	0.500	0.020	100.000
19	WAAW waw station	13	0.500	0.020	100.000

5	DGAR Diego Garcia	elevation	8.50	9.69
6	GYBU gyophu stati	elevation	5.95	6.12
7	HAKA hakha statio	elevation	5.61	4.42
8	IGLE ingle statio	elevation	12.07	10.03
9	IISC Indian Insti	elevation	6.97	4.93
10	KANI kanni statio	elevation	15.13	8.67
11	LCK2 Lucknow(Utta	elevation	6.63	5.95
12	LHAZ Lhasa	elevation	7.31	4.25
13	NTUS Nanyang Tech	elevation	7.31	4.25
14	PERT Perth	elevation	6.97	5.44
15	PIMO Manila Obser	elevation	3.40	6.80
16	SATG shanatetg st	elevation	85.00	0.00
17	SDWN seldwin stat	elevation	5.61	4.42
18	SWBO shewbo stati	elevation	5.44	0.00
19	WAAW waw station	elevation	13.94	8.16

#####

End of tight solution with LC observable and ambiguities fixed

 Performing LC biases-free loose solution

A priori coordinate errors in kilometers

	Latitude	Longitude	Radius
1	BAKO BAKOSURTANAL	0.01000	0.01000 0.01000
2	COCO Cocos	0.01000	0.01000 0.01000
3	CUSV Chulalongkor	0.01000	0.01000 0.01000
4	DARW Darwin AU014	0.01000	0.01000 0.01000
5	DGAR Diego Garcia	0.01000	0.01000 0.01000
6	GYBU gyophu stati	0.01000	0.01000 0.01000
7	HAKA hakha statio	0.01000	0.01000 0.01000
8	IGLE ingle statio	0.01000	0.01000 0.01000
9	IISC Indian Insti	0.01000	0.01000 0.01000
10	KANI kanni statio	0.01000	0.01000 0.01000
11	LCK2 Lucknow(Utta	0.01000	0.01000 0.01000
12	LHAZ Lhasa	0.01000	0.01000 0.01000
13	NTUS Nanyang Tech	0.01000	0.01000 0.01000
14	PERT Perth	0.01000	0.01000 0.01000
15	PIMO Manila Obser	0.01000	0.01000 0.01000

16 SATG shanatetg st	0.01000	0.01000	0.01000
17 SDWN seldwin stat	0.01000	0.01000	0.01000
18 SWBO shewbo stati	0.01000	0.01000	0.01000
19 WAAW waw station	0.01000	0.01000	0.01000

A priori zenith-delay errors in meters

1 BAKO BAKOSURTANAL	0.500	0.020	100.000
2 COCO Cocos	0.500	0.020	100.000
3 CUSV Chulalongkor	0.500	0.020	100.000
4 DARW Darwin AU014	0.500	0.020	100.000
5 DGAR Diego Garcia	0.500	0.020	100.000
6 GYBU gyophu stati	0.500	0.020	100.000
7 HAKA hakha statio	0.500	0.020	100.000
8 IGLE ingle statio	0.500	0.020	100.000
9 IISC Indian Insti	0.500	0.020	100.000
10 KANI kanni statio	0.500	0.020	100.000
11 LCK2 Lucknow(Utta	0.500	0.020	100.000
12 LHAZ Lhasa	0.500	0.020	100.000
13 NTUS Nanyang Tech	0.500	0.020	100.000
14 PERT Perth	0.500	0.020	100.000
15 PIMO Manila Obser	0.500	0.020	100.000
16 SATG shanatetg st	0.500	0.020	100.000
17 SDWN seldwin stat	0.500	0.020	100.000
18 SWBO shewbo stati	0.500	0.020	100.000
19 WAAW waw station	0.500	0.020	100.000

A priori atmospheric gradient error at 10 degrees elevation angle

Station	#	N/S: A priori(m)	Mar(m/sqrt(hr))	Correl(hr)	E/W: A priori(m)	Mar(m/sqrt(hr))	Correl(hr)
1 BAKO BAKOSURTANAL	2	0.01000	0.01000	100.0	0.01000	0.01000	100.0
2 COCO Cocos	2	0.01000	0.01000	100.0	0.01000	0.01000	100.0
3 CUSV Chulalongkor	2	0.01000	0.01000	100.0	0.01000	0.01000	100.0
4 DARW Darwin AU014	2	0.01000	0.01000	100.0	0.01000	0.01000	100.0
5 DGAR Diego Garcia	2	0.01000	0.01000	100.0	0.01000	0.01000	100.0
6 GYBU gyophu stati	2	0.01000	0.01000	100.0	0.01000	0.01000	100.0
7 HAKA hakha statio	2	0.01000	0.01000	100.0	0.01000	0.01000	100.0
8 IGLE ingle statio	2	0.01000	0.01000	100.0	0.01000	0.01000	100.0
9 IISC Indian Insti	2	0.01000	0.01000	100.0	0.01000	0.01000	100.0
10 KANI kanni statio	2	0.01000	0.01000	100.0	0.01000	0.01000	100.0

11	LCK2	Lucknow(Utta	2	0.01000	0.01000	100.0	0.01000	0.01000	100.0
12	LHAZ	Lhasa	2	0.01000	0.01000	100.0	0.01000	0.01000	100.0
13	NTUS	Nanyang Tech	2	0.01000	0.01000	100.0	0.01000	0.01000	100.0
14	PERT	Perth	2	0.01000	0.01000	100.0	0.01000	0.01000	100.0
15	PIMO	Manila Obser	2	0.01000	0.01000	100.0	0.01000	0.01000	100.0
16	SATG	shanatetg st	2	0.01000	0.01000	100.0	0.01000	0.01000	100.0
17	SDWN	seldwin stat	2	0.01000	0.01000	100.0	0.01000	0.01000	100.0
18	SWBO	shewbo stati	2	0.01000	0.01000	100.0	0.01000	0.01000	100.0
19	WAAW	waw station	2	0.01000	0.01000	100.0	0.01000	0.01000	100.0

**** Summary of biases-free solution ****

Total parameters: 1364 live parameters: 843
 Prefit nrms: 0.15149E+01 Postfit nrms: 0.19494E+00
 – Uncertainties not scaled by nrms
 End of loose solution with LC observable and ambiguities free

Performing LC biases-fixed loose solution

**** Summary of biases-fixed solution ****

Total parameters: 1364 live parameters: 475
 Prefit nrms: 0.15112E+01 Postfit nrms: 0.19858E+00
 – Uncertainties not scaled by nrms
 End of loose solution with LC observable and ambiguities fixd

Normal stop in SOLVE

Appendix E: Track command

```
*
* To use this command file the -d and -w options must used in the
* runstring:
* track -f track.cmd -d 316 -w 17140
*-----
* OBS_FILE
* Give the rinex file names to be processed, The obs_file command
* must be given first. At least one site must be named as F which
* means the position of the site is fixed. It recommended to have
* only one fixed site. The other sites are denoted K for kinematic.
* The site_stats command determines if a site position will be able
* to change during the processing.
* NOTE: At least one blank line must follow the last station in
* the list and there can be no blank lines between the station
* list.
obs_file
# all process relative to LHAZ
lhaz lhaz3160.12o F
swbo swbo3160.12o K
sdwn sdwn3160.12o K
*-----
* NAV_FILE
* An orbit file must be given.
* NOTE: when 24-hours of data are processed the sp3 files from
* day before and after need to be concatenated with the sp3 file
* from the day being processed to ensure that there are ephemeris
* entries before and after the last data points. A simple unix
* cat command can be used to generate the merged files.
nav_file igs17140.sp3 SP3
#SITE_POS (by default, it takes the coord. from rinex files)
*-----
site_pos
lhaz -106941.43662 5549269.87743 3139215.00618
swbo -587090.26669 5863185.54404 2433085.00489
sdwn -628038.65628 5858357.27111 2434529.29578
```

```

*-----
* MODE <Type>
* The MODE command allows the setting of defaults for the type of
* data being processed. These setting can then be overwritten if
* desired by use of the commands below. Three default setting modes
* are supported for <Type>:
* AIR - Assumed to be high-sample rate aircraft. Sets the search_type to
*       L1+L2, and allows gaps of 4-epochs, and minimum data of 120 epochs
*       (1 minute for 2Hz data).
* SHORT - Short baseline static data (<1 km). Sets search and analysis type
*         to L1+L2 and minimum data of 20 epochs (10 minutes of 30 second
*         sampled data). Data is still processed as kinematic data.
* LONG - Long baseline static data (>1 km). Sets search and analysis type
*        to LC and minimum data of 20 epochs. Atmospheric delay estimation
*        is turned on with 0.1 m apriori sigma, and process noise variance
*        of 1.d-6 m**2/epoch (~1 mm changes every 30 seconds for 30 second
*        sampled data which accumulates to +-5 cm in a day). These settings
*        are the same as atm_stats 0.1 0.001
mode long
*----- <END of required inputs> -----
* The commands below are optional and are used to specific output
* files and change some defaults
*-----
* Specific day specific output files
pos_root TRAK<day>
res_root TRAK<day>
sum_file TRAK<day>.sum
*-----
* INTERVAL <seconds>
* Allows specification of sampling interval. Must be in integer multiple
* of actual sampling interval (Units: seconds)
* NOTE: When rinex files have different sampling the largest interval
* should be specified. I may also be necessary to give a start_time
* to have the epoch line up correct (**DISASTER** No matching data
* message).
* If the sampling interval is in the rinex files this is not needed

```

* unless a longer sampling interval is desired
interval 1
*-----

* Select the output coordinate type. For quick assessment and
* looking at relative motions North, East and Up (all in meters)
* are convenient
* Use NEU+GEOD to get both NEU output and geodetic lat, long and height.
* Use GEOD to get just geodetic coordinates.
out_type NEU
*-----

* SITE_STATS
* Site <Apriori Sigma in XYZ> <RW noise in XYZ>
* Gives statistics to assign to the kinematic station positions.
* The <Apriori Sigma in XYZ> are the three sigmas in XYZ for the
* initial position and <RW noise in XYZ> are the three sigmas in XYZ
* for the change in position between epochs of data. Since the
* motion of the kinematic sites is modeled as random walk (RW), the
* sigma of the change in position grows as the sqrt(number of epochs)
* ALL can be used for the station name and the same statistics will
* be applied to all kinematic sites (NOTE: the fixed site do not
* change position).
* e.g.
* site_stats
* all 20 20 20 10 10 10
* (20 meters apriori sigmas and changes of 10 meters between epochs).
*
* For static sites on long baselines (>50 km), fixing the
* station coordinates to good apriori values can often be used
* to get better ranking in the LC search. This can be done by
* using site_stats 0.0001 0.0001 0.0001 1 1 1. In the way
* track does its searches, the apriori sigma of 0.1 mm (in this
* case) would be used during the search, but in the final output
* the markov process noise of 1 m would be applied at each epoch
* (except the first). Once the ambiguities are resolved and an
* ambin file generated, the solution could be re-run with loose
* aprioris sigmas.

site_stats

all 0.15 0.15 0.15 0.025 0.025 0.025

* all 0.01 0.01 0.01 0.01 0.01 0.01

*-----

* BACK_TYPE <string>

* Allows specification of the type of solution to run backwards in time.

* Current options are (vers 1.02)

* BACK -- Simply runs a standard KF backwards in time. Write both the

* forward and backwards solution to the output file.

* Options for vers =>1.03

* SMOOTH -- runs a smoothing filter. Only the forward running epochs

* are written to the output file.

* Running the smoothing filter is recommended on long baselines

* because this uses all the data for atmospheric delay estimation

* and any non-integer biases (non-resolved biases) are constant

back_type smooth

*-----

* FLOAT_TYPE <Start> <Decimation> <Type> <Float sigma Limits(2)> <WL_Fact> <lon_fact> <MAX_Fit>

* Allows specification of the floating point ambiguity limits. It is

* through this command that the bias fixing algorithm is controlled.

* The main factors to consider are the <WL_Fact> and <lon_fact> values

* which default to 1 giving them equal weight with the fit of the LC

* data. (For L1+L2 float type, these entries are ignored).

* For long baselines (>20 km) the <lon_fact> should be reduced

* to give less weight to the ionospheric delay constraint. For 100 km

* baselines, 0.1 seems to work well. With very good range data (ie.,

* WL ambiguities all near integer values), this factor can be

* reduced.

* For noisy or systematic range data (can be tested with a P1,P2 or PC

* solution), the WL_fact may be reduced.

* <Start> is the iteration to start the floating point estimation

* (default is 1)

* <Decimation> is decimation level ie. how often should the data

* be sampled in making the estimate (default is 4)

* <Type> Data type to use for the estimate. Choices are

* L1+L2 or LC. Note: for LC ambiguity resolution, the

```

*      MW-Widelanes need to be well determined so that the
*      L1-L2 ambiguities can be resolved from these estimates
*      <Float sigma Limits(2)> Limits in the standard deviation of the
*      floating point estimate that allows it to be fixed to
*      an integer value (cycles), and on the maximum sigma
*      allowed even to attempt resolving biases (Two values
*      are needed). The sigma of the estimate
*      will depend on the data noise assumed and the
*      decimation rate (defaults are 0.25 cycles and 0.5 cycles)
*      <WL_Fact> weight to be given to deviation of MW-WL from zero.
*      Default is 1 (ie., equal weight with LC residuals).
*      Setting the value smaller will downweight the contribution
*      of the MW-WL
*      <lon_fact> weight to be given to deviation of the Ionospheric delay
*      from zero. Default is 1 (i.e., ionospheric delay is assumed
*      to be zero and given unit weighting in determining how
*      well a set of integer ambiguities fit the data. On long
*      baselines, value should be reduced.
*      <MAX_Fit> Maximum value of (res/sig)**2 allowed for biases to be
*      fixed. (Default 25).
*
* Small changes to the default parameters to resolve more bias
* parameters for this data.
* float_type 1 1 LC 0.25 0.5 1 0.01 25
* ion_stats 0.5 5 0.01 350 300
*-----
* BF_SET <Max gap> <Min good>
* Allows specification of the maximum size of gap allowed in data before
* a bias flag is inserted, and the number of good data needed to allow
* data to be kept. The defaults are 1 and 20 (i.e., any gap is flagged
* and at least 20 good phase measurements are needed between bias flags
* other wise the data is deleted).
* For high rate, telemetered data there are often gaps due to missed
* telemeter. For this data set, these gaps are less than 2-seconds
* and here we set gap size before a bias parameter is added to 2-seconds.
** bf_set 10 60

```

```

* bf_set 2 60
*-----
* ATM_STATS
* Site <Apriori Zenith delay sigma> <RW noise in Zenith delay>
* Gives the statistics for the atmospheric delays by site. The values
* are the initial sigma in meters and RW changes in meters.
* e.g.,
* atm_stats
*   t39a  0.1 0.001
* Set the apriori sigma as 10cm and allows the delay to change 1mm every
* epoch.
** atm_stats
**   ovll  0.1 0.1
**   bton  0.1 0.1
**   lsch  0.1 0.1
* atm_stats
*   ovll  1.1 1.1
*   bton  1.1 1.1
*   lsch  1.1 1.1
*-----
* ATM_BIAS
* Site <Atmospheric delay offset (m)>
* Allows adjustment to the apriori atmospheric delay model. Value is added
* to the nominal delay. In track Version 1.0, only a single offset applied to
* all epochs can be specified. Command is most appropriate for static sites
* separated by more than 20 km.
*
* ATM_FILE <File name>
* Allows the specification of file containing total atmospheric delay estimates
* at each site. The file format is the same as that obtained by grep'ing
* on 'ATM_ZEN X' in the o-file from a gamit run.
*
* For static baselines with site separations of >50km, the
* differential atmospheric (ie., difference from the apriori
* atmospheric delay model) can be large due to water vapor. The
* ATM_BIAS command be used to compensate for this difference and

```

- * this will often allow the biases to be fixed. (The value chosen
- * can be based on the part of the data where the biases were
- * fixed or on another geodetic analysis e.g. a standard gamit
- * solution.) In static solution, differential atmospheric
- * delays of 10 cm at zenith (38 cm at 15 deg --- equivalent to
- * 2 cycles) are often seen.



GLOSSARY

- cGPS – continuous Global Positioning System
- DGPS – Differential Global Positioning System
- DoD - US Department of Defense
- DORIS - Doppler Orbitography and Radiopositioning Integrated by Satellite
- EOPs - Earth Orientation Parameters
- EOS - Earth Observatory of Singapore
- EX-WL - Extra wide lane Linear Combination
- GAMIT - Programs for the analysis of GPS data
- GGMatlab – Program for viewing GPS velocities and time series
- GLOBK - Program for combining various geodetic solutions
- GNSS – Global Navigation Satellite System
- GMT - Generic mapping tool
- GLONASS - GLObal NAVigation Satellite System
- GPS - Global Positioning System
- ICRF - International Celestial Reference Frame
- IERS - International Earth Rotation and Reference Systems Service
- IGS - International GNSS Service
- ITRF - International Terrestrial Reference Frame
- ITRS - International Terrestrial Reference System
- L1 - L-band signal (1572.42 MHz)
- L2 - L-band signal (1227.60 MHz)
- LC - Linear Combination
- LG - geometry-free combination
- NAVSTAR - Navigation Satellite Timing and Ranging.
- MEC – Myanmar Earthquake Committee
- MCS - Master Control Station
- MIT - Massachusetts Institute of Technology

MW-WL - Melbourne-Wubben wide lane combination

RINEX - Receiver Independent Exchange format

RMS - Root Mean Square

SLR - Satellite Laser Ranging

SOPAC - Scripps Orbits and Permanent Array Center

TEQC - Translate, Edit, and Quality Check, is software developed and maintained by UNAVCO

TRACK – program developed by MIT for kinematic GPS processing

UTC- Universal Time Coordinated

WL – wide lane

VLBI - Very Long Baseline Interferometry



VITA

Mr. PYAE SONE AUNG was born in Meikhtila, Myanmar, on May 22, 1988. He received Bachelor of Engineering (Mechatronic Engineering) in 2010 from Department of Mechatronic Engineering, Hmawbi University in Myanmar. He worked as a volunteer for three years in a non-government organization, Myanmar Earthquake Committee, Myanmar Engineering Society. He started as a Master's student in the department of Survey, faculty of Engineering, Chulalongkorn University in 2013 and completed in May 2015.

Publication List

1. Conference presentation

- Sone Aung .P, Satirapod .C, Monitoring of the Sagaing fault in Myanmar using GPS observations. GeolInfotech 2014. Bangkok, Nov. 12-14, 2014.

